Adaptive Neural Network-Based Event-Triggered Control of Single-Input Single-Output Nonlinear Discrete-Time Systems

Avimanyu Sahoo, Hao Xu, *Member, IEEE*, and Sarangapani Jagannathan, *Senior Member, IEEE*

***Abstract*— This paper presents a novel adaptive neural network (NN) control of single-input and single-output uncertain nonlinear discrete-time systems under event sampled NN inputs. In this control scheme, the feedback signals are transmitted, and the NN weights are tuned in an aperiodic manner at the event sampled instants. After reviewing the NN approximation property with event sampled inputs, an adaptive state estimator (SE), consisting of linearly parameterized NNs, is utilized to approximate the unknown system dynamics in an event sampled context. The SE is viewed as a model and its approximated dynamics and the state vector, during any two events, are utilized for the event-triggered controller design. An adaptive event-trigger condition is derived by using both the estimated NN weights and a dead-zone operator to determine the event sampling instants. This condition both facilitates the NN approximation and reduces the transmission of feedback signals. The ultimate boundedness of both the NN weight estimation error and the system state vector is demonstrated through the Lyapunov approach. As expected, during an initial online learning phase, events are observed more frequently. Over time with the convergence of the NN weights, the inter-event times increase, thereby lowering the number of triggered events. These claims are illustrated through the simulation results.**

***Index Terms*— Adaptive control, event-triggered control (ETC), function approximation, neural network (NN) control.**

I. INTRODUCTION

TRADITIONAL periodic transmission of feedback control signals in a closed-loop networked environment requires a higher network bandwidth. Event-triggered control (ETC) [1]–[12], on the other hand, is emerged recently as an alternate method to reduce the network communication and controller execution. In ETC, the aperiodic sampling of system state vector is proved to be advantageous computationally over periodic sampled control schemes [1].

The ETC technique allows the system errors to increase to a predefined threshold before transmitting the feedback signals. The threshold is designed to both avoid instability and meet a certain desired performance. Therefore, the transmissions of the feedback signals and the control input are reduced while achieving a desired control performance. These transmission instants are usually referred to as event sampled instants or simply event-trigger instants [2]. The condition under which a decision is made to transmit the feedback and control signals is known as event-trigger condition [2]. The event-trigger condition is normally a function of the system state error, which is referred to as event-trigger error [2]–[9] along with a state-dependent threshold.

Tabuada [2], on ETC, assumed input-to-state stability of the system with respect to the event-trigger error for designing an event-trigger condition. It was shown that the event-based controller ensured the asymptotic stability of the system with reduced computation. Later, various other ETC schemes [3]–[12] are developed for both linear and nonlinear systems. A majority of these ETC schemes are implemented by using a zero-order-hold (ZOH) [2], [3] in order to maintain both the last transmitted state vector and control input until the next transmission.

An alternate to the ZOH scheme is the model-based scheme [5], [6], [8] where the state vector from a model is used to generate the control input within any two event-trigger instants. The model-based approach is shown to reduce network traffic more than a ZOH-based scheme at the expense of an additional computation due to the model. However, in all the ETC effort [2]–[8], the system dynamics are considered available *a priori*, while a small bounded uncertainty can be tolerated [6]. In contrast, in our preliminary work, adaptive model-based schemes [10], [11] both for uncertain linear systems and partially unknown nonlinear systems, respectively, were introduced.

From the stability point of view and to account for the aperiodic transmissions of the feedback signals, several closed-loop modeling techniques are also presented. A representative list includes the piecewise linear system model [8], the perturbed system model [6], the hybrid dynamical system model, and impulsive dynamical system model [8]. All these modeling approaches utilized the Lyapunov method or its extension for the stability analysis and to design the event-trigger condition.

In this paper, an adaptive model-based ETC scheme for a nonlinear discrete-time system in Brunovsky canonical form is presented. Both the internal dynamics and the control coefficient function are considered unknown. By using the approximation property of neural networks (NNs) [16], in an event sampled context, an adaptive state estimator (SE) is

Manuscript received July 23, 2013; revised June 7, 2015; accepted August 13, 2015. Date of publication October 26, 2015; date of current version December 17, 2015. This work was supported in part by the National Science Foundation under Grant ECCS 1406533 and in part by the Intelligent Systems Center, Missouri University of Science and Technology, Rolla, MO, USA.

A. Sahoo and S. Jagannathan are with the Department of Electrical and Computer Engineering, Missouri University of Science and Technology, Rolla, MO 65409 USA (e-mail: asww6@mst.edu; sarangap@mst.edu).

H. Xu is with the Department of Electrical Engineering, College of Science and Engineering, Texas A&M Corpus Christi, Corpus Christi, TX 78412 USA (e-mail: hao.xu@tamucc.edu).

Color versions of one or more of the figures in this paper are available online at http://ieeexplore.ieee.org.

Digital Object Identifier 10.1109/TNNLS.2015.2472290

designed. The adaptive SE serves as a model of the system and both approximates the system dynamics and estimates the state vector. The approximated system dynamics and the estimated state vector are subsequently utilized for generating the control input, during any two event sampled instants.

A novel event-trigger condition is derived using the Lyapunov method of stability. The threshold in the event-trigger condition is designed as a function of both the NN weight estimates and the system state vector. Thus, the threshold becomes adaptive unlike the traditional threshold conditions [2]–[5], which are the functions of system state vector alone. This modified adaptive event-trigger condition not only ensures the function approximation using a nonperiodic weight update law but also the stability. The event-trigger condition further uses a dead-zone operator to prevent the unnecessary triggering of events, due to the NN reconstruction error, once the system state is inside the ultimate bound.

The contributions of this paper include: 1) the event sampled NN approximation with model state vector; 2) the development of a novel model-based adaptive NN ETC scheme; 3) an aperiodic tuned NN-based SE or model; and 4) an adaptive event-trigger condition to ensure the stability and the convergence of NN weight estimates.

The completely uncertain system dynamics make the event-trigger condition design different from the traditional ones [2]–[6], including partially unknown dynamics in [11]. The stability of the event-triggered closed-loop system is proved by using the idea of switched systems, as discussed in [7] and [13]. The Lyapunov function is allowed to increase during the inter-event times but bounded. It is shown that the bound for the Lyapunov function during inter-event times converges to the ultimate value with events occurring. This enables the proposed NN-based adaptive event-triggered scheme to ensure stability in the presence of a significant level of dynamic uncertainty. It also reduces the network traffic with fewer numbers of triggered events when compared with a traditional discrete-time systems.

The remaining part of this paper is organized as follows. Section II revisits the event-based approximation and formulates the problem for the ETC of uncertain dynamical systems. Section III details the design procedure for the NN-based adaptive ETC. The stability is claimed in Section IV. The simulation results are presented in Section V. Finally, the conclusion is drawn in Section VI. The Appendix details the proofs for the lemmas and the theorems.

II. Background and Problem Formulation

This section presents a brief background on the traditional ETC and formulates the problem for adaptive ETC.

A. Background on ETC

Consider a controllable nonlinear uncertain discrete-time system in Brunovsky canonical form given by

$$\begin{aligned} x_{1,k+1} &= x_{2,k} \\ x_{2,k+1} &= x_{3,k} \\ &\vdots \\ x_{n,k+1} &= f(x_k) + g(x_k)u_k \\ y_k &= x_{1,k} \end{aligned} \tag{1}$$

where $x_k = [x_{1,k}\ x_{2,k}\ \ldots\ x_{n,k}]^T \in \Re^n$, $u_k \in \Re$, and $y_k \in \Re$ denote the state vector, the input, and the output of the system. The internal dynamics and the control coefficient function, $f : \Re^n \to \Re$ and $g : \Re^n \to \Re$, respectively, are the unknown nonlinear smooth functions. The system is considered to be feedback linearizable in the sense that there exists a diffeomorphism to transform the system into a linear form.

System (1) can be written in simplified form as

$$x_{k+1} = Ax_k + Bf(x_k) + Bg(x_k)u_k \tag{2}$$

where

$$A = \begin{bmatrix} 0 & 1 & \cdots & 0 \\ 0 & 0 & \ddots & 0 \\ \vdots & \vdots & \ddots & 1 \\ 0 & 0 & 0 & 0 \end{bmatrix} \in \Re^{n\times n}$$

and $B = [0\ 0\ \cdots\ 1]^T \in \Re^n$. The system dynamics (2) can be rewritten in a compact form as

$$x_{k+1} = Ax_k + B\bar{F}(x_k)\bar{u}_k \tag{3}$$

where $\bar{F}(x_k) = [f(x_k)\ g(x_k)] \in \Re^{1\times 2}$ and $\bar{u}_k = [1\ u_k]^T \in \Re^2$ are the augmented system dynamics and the input vector, respectively. These augmented forms are utilized in the model development and the controller design. To design a controller by using feedback linearization, the following assumption is required.

Assumption 1 [14]: The nonlinear function $g(x_k)$ is lower bounded. Without the loss of generality, $g(x_k)$ is assumed to satisfy $0 < g_{\min} \le |g(x_k)|$, where $g_{\min}$ is a known positive constant and $|\cdot|$ denotes the absolute value.

For system (1), under the complete knowledge of system dynamics, a feedback linearizable controller of the following form:

$$u_{d_k} = (-f(x_k) + v_k)/g(x_k) \tag{4}$$

yields an asymptotically stable closed-loop system. The closed-loop dynamics can be written as

$$x_{k+1} = A_c x_k \tag{5}$$

where u_{d_k} is the ideal control input. The stabilizing control input is given by $v_k = Kx_k$, where $K = [K_1\ K_2\ \cdots\ K_n]$ is the control gain vector. The control gain vector $K \in \Re^{1\times n}$ can be designed to ensure A_c is Schur through a suitable pole placement design. The closed-loop system matrix can be written as

$$A_c = A + BK = \begin{bmatrix} 0 & 1 & \cdots & 0 \\ 0 & 0 & \ddots & \vdots \\ \vdots & \ddots & \ddots & 1 \\ K_1 & K_2 & \cdots & K_n \end{bmatrix} \in \Re^{n\times n}.$$

For the class of systems given by (1), any nonlinear controller can also be utilized, which renders the asymptotic stability of the system. The ideal controller (4) needs time-based periodic sampled system state x_k for implementation along with $f(x_k)$ and $g(x_k)$. In contrast, our main objective in this paper is to implement the controller (4) in the event sampled context without the knowledge of the system dynamics.

In the case of the traditional ETC, the system state vector x_k is transmitted to the controller only at the event sampled instants. Define a subsequence $\{k_i\}_{i=1}^{\infty}$ of the discrete sequence of time instants $k \in \mathbb{N}$, referred to as event sampled instants. The events are triggered at k_i, $\forall\ i \in \mathbb{N}$ with the first event occurring at the time instant $k_0 = 0$. The system state vector, x_{k_i}, is transmitted through the communication network and held by a ZOH until the next transmission at k_{i+1}. The last held state, x_{k_i} for $k_i \leq k < k_{i+1}$ at the ZOH is piecewise constant and used for the controller implementation.

The event sampled instants are determined at the trigger mechanism by evaluating the event-trigger error against the threshold value. The deviation between x_k and the last transmitted state x_{k_i} is usually referred to as the event-trigger error, e_k^{ET}. This is represented as

$$e_k^{\mathrm{ET}} = x_k - x_{k_i}, \quad k_i \leq k < k_{i+1}, \quad i \in \mathbb{N}. \tag{6}$$

Though event-trigger condition is evaluated periodically at all $k \in \mathbb{N}$, the state vector is transmitted to the controller only at the event sampled instants determined by the event-trigger condition.

Now, to implement the controller (4), the unknown system dynamics, $f(x_k)$ and $g(x_k)$, must be approximated by using event sampled system state vector, x_{k_i}. Therefore, the universal approximation property of the NN is revisited for the event-based sampling in Section II-B.

B. Problem Formulation

The problem of ETC is formulated in this section by addressing event sampled NN approximation and transmission of state vector.

1) Event Sampled NN Approximation: According to the universal approximation property [16] of the NN, a nonlinear smooth function $h(x_k) \in \Re^n$ can be approximated in a compact set for all $x_k \in \Omega_x \subset \Re^n$. A linearly parameterized NN [16] with one hidden layers can be used for the purpose. The two layer NN can consist of a layer of randomly assigned constant weights, V_h, in the input layer and tunable weight matrix, W_h, in the output layer. It has been proved that by randomly selecting the input layer weights, the activation function forms a stochastic basis [16]. Thus, the NN approximation property holds [16] for all inputs x_k belong to a compact set Ω_x. The function $h(x_k) \in \Omega_x$ with the linearly parameterized NN can be represented as

$$h(x_k) = W_h^T \psi_h\left(V_h^T x_k\right) + \varepsilon_h(x_k) \tag{7}$$

where $W_h \in \Re^{l \times n}$ is the NN target weight matrix. The randomly assigned input weight matrix is denoted by $V_h \in \Re^{n \times l}$, and $\psi_h(\cdot) \in \Re^l$ is the activation function vector. The NN reconstruction error and the number of hidden layer neurons are denoted by $\varepsilon_h(x_k) \in \Re^n$ and l, respectively. So far in the literature, the universal NN approximation property considers the availability of x_k periodically at all-time instants k.

In the case of an ETC, the approximation of the function at event sampled instants $h(x_{k_i})$ can be expressed as [12]

$$h(x_{k_i}) = W_h^T \psi_h\left(V_h^T x_{k_i}\right) + \varepsilon_h(x_{k_i}) \tag{8}$$

where $\psi_h(V_h^T x_{k_i}) \in \Re^l$ is the activation function with event sampled state vector, x_{k_i}. The reconstruction error at event sampled instants is given by $\varepsilon_h(x_{k_i}) \in \Re^n$. Note that the approximations (7) and (8) become equal if the events are triggered at all-time instants. Since the events are occurring in an aperiodic manner, the function $h(x_k)$ for $k_i \leq k < k_{i+1}$ can be expressed as

$$\begin{aligned} h(x_k) = W_h^T \psi_h\left(V_h^T x_{k_i}\right) + \varepsilon_{h,e}\left(x_{k_i}, e_k^{\mathrm{ET}}\right)& \\ k_i \leq k < k_{i+1}, \quad i \in \mathbb{N}& \end{aligned} \tag{9}$$

where $\varepsilon_{h,e}(x_{k_i}, e_k^{\mathrm{ET}})$ is the event sampled reconstruction error computed next.

Consider the periodic approximation of the function $h(x_k)$ as in (7). By adding and subtracting $\psi_h(V_h^T x_{k_i})$ and definition (6), it can be rewritten as

$$\begin{aligned} h(x_k) &= W_h^T \psi_h\left(V_h^T x_k\right) + W_h^T \psi_h\left(V_h^T x_{k_i}\right) \\ &\quad - W_h^T \psi_h\left(V_h^T x_{k_i}\right) + \varepsilon_h(x_k) \\ &= W_h^T \psi_h\left(V_h^T x_{k_i}\right) + W_h^T\left(\psi_h\left(V_h^T\left(x_{k_i} + e_k^{\mathrm{ET}}\right)\right)\right. \\ &\quad \left.- \psi_h\left(V_h^T x_{k_i}\right)\right) + \varepsilon_h\left(x_{k_i} + e_k^{\mathrm{ET}}\right) \\ &\qquad\qquad k_i \leq k < k_{i+1} \quad \forall i \in \mathbb{N}. \end{aligned} \tag{10}$$

Comparing (9) and (10), the event sampled NN reconstruction error $\varepsilon_{h,e}(x_{k_i}, e_k^{\mathrm{ET}}) = \varepsilon_h(x_{k_i} + e_k^{\mathrm{ET}}) + W_h^T(\psi_h(V_h^T(x_{k_i} + e_k^{\mathrm{ET}})) - \psi_h(V_h^T x_{k_i}))$.

The event sampled NN reconstruction error, $\varepsilon_{h,e}(x_{k_i}, e_k^{\mathrm{ET}})$, is a function of the traditional NN reconstruction error $\varepsilon_h(x_k) = \varepsilon_h(x_{k_i} + e_k^{\mathrm{ET}})$ as in (7) and an additional error due to event sampled input, i.e., $W_h^T(\psi_h(V_h^T(x_{k_i} + e_k^{\mathrm{ET}})) - \psi_h(V_h^T x_{k_i}))$. This additional error is a function of event sampled state vector, x_{k_i}, and the event-trigger error e_k^{ET}. Therefore, to approximate a function with a desired level of accuracy in an ETC context, the event-trigger error, e_k^{ET}, must be kept small. This can be achieved by designing a suitable event-trigger condition. Higher is the number of event sampled instants, better will be the NN approximation. However, this will increase the number of transmissions leading to higher network bandwidth usage.

The NN estimation of the function $\hat{h}(x_k)$ for $k_i \leq k < k_{i+1}$, $\forall i \in \mathbb{N}$ can be written as

$$\begin{aligned} \hat{h}(x_k) &= \hat{W}_{h,k}^T \psi_h\left(V_h^T x_k\right) \\ &= \hat{W}_{h,k}^T \psi_h\left(V_h^T x_{k_i}\right) + \hat{W}_{h,k}^T\left(\psi_h\left(V_h^T\left(x_{k_i} + e_k^{\mathrm{ET}}\right)\right)\right. \\ &\qquad \left.- \psi_h\left(V_h^T x_{k_i}\right)\right) \end{aligned} \tag{11}$$

where $\hat{W}_{h,k} \in \Re^{l \times n}$ is the NN weight estimate. The second term $\hat{W}_{h,k}^T(\psi_h(V_h^T(x_{k_i} + e_k^{\mathrm{ET}})) - \psi_h(V_h^T x_{k_i}))$ is an additional error in estimation and a function of the event-trigger error.

It is important to mention here that the event-based aperiodic transmission precludes the traditional periodic NN weight update [16]. The NN weights must be tuned in an aperiodic manner only at the event sampled instants, $k = k_i$ with the

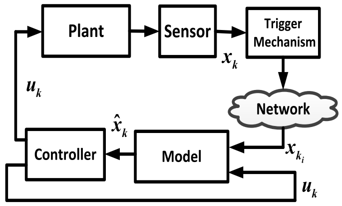

Fig. 1. Structure of the traditional MBETC system.

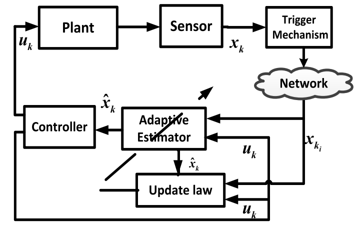

Fig. 2. Structure of the adaptive MBETC system.

latest measuring state vector. This, further, requires a suitable event-trigger condition to maintain estimation accuracy.

From the above discussion, the accuracy of NN approximation, the reduction in transmissions, and the system stability depend upon the event-trigger condition. Thus, a tradeoff must be reached through a careful design of the event-trigger condition. As a solution, the threshold of the event-trigger condition is made adaptive in contrast with the fixed threshold utilized in the traditional ETC design with known dynamics [2], [3].

An alternate to this ZOH-based technique is the model-based approach, as discussed in Section II-B2.

2) Model-Based ETC: The structure of a model-based ETC (MBETC) scheme [5], [6], [8] is shown in Fig. 1.

Traditionally, a system model (known *a priori*) generates the state vector between the event sampled instants. The model state vector is subsequently used by the controller to update the control input periodically in contrast with a ZOH ETC. The event sampled instants are determined by the deviation of the model state from the measured system state vector due to model uncertainty or disturbance. The measured system state vector is transmitted at the event sampled instants to reinitialize the model state vector.

The event-trigger error for an MBETC scheme can be redefined as the difference between the measured system state and the model state vector. It is given by

$$e_k^s = x_k - \hat{x}_k, \quad k_i \le k < k_{i+1} \quad \forall i \in \mathbb{N} \tag{12}$$

where $\hat{x}_k \in \Re^n$ is the model state vector. The reinitialized model state vector at the trigger instants can be represented as

$$\hat{x}_k = x_k, \quad k = k_i \quad \forall i \in \mathbb{N} \tag{13}$$

and then, it evolves with model dynamics during the inter-event times for $k_i < k < k_{i+1}$. Since the system dynamics in (1) are uncertain, the traditional model-based ETC framework cannot be directly used. This requires an adaptive NN scheme to construct the model or SE. Furthermore, the model dynamics must also be approximated in the MBETC context similar to the ZOH-based case as discussed before. The detailed design procedure is presented in Section III.

III. Model-Based Adaptive ETC Design

The adaptive MBETC scheme for an uncertain nonlinear discrete-time system is proposed in this section. We assume a communication network between the sensor and the controller but without packet losses and delays. This assumption is consistent with the ETC literature [8] for the purpose of controller design.

The structure of the traditional MBETC, shown in Fig. 1, is modified for an adaptive MBETC and shown in Fig. 2. An NN-based adaptive model or SE is included not only to estimate the state vector but also to approximate the unknown system dynamics. An adaptive event-trigger condition is also proposed using the SE's estimated NN weights and the system state. Therefore, a mirror SE at the trigger mechanism is used to evaluate the event-trigger condition. This mirror SE estimates the NN weights locally at the trigger mechanism to avoid the transmission of the NN weight estimates through the communication network. The mirror SE operates in synchronism with the SE at the controller. At the trigger instant $k = k_i$, the system state x_{k_i} and x_{k_i-1}, are transmitted together. The received state vectors are used to update the NN weights at trigger instants in an aperiodic manner. Then, the event-trigger error, e_k^s, in (12) is reset to zero for the next cycle of triggering. The detailed design procedure for the NN-based adaptive MBETC scheme is presented next.

A. Adaptive Estimator and Controller Design

The dynamics of the adaptive SE can be expressed as

$$\hat{x}_{k+1} = A\hat{x}_k + B\hat{f}(\hat{x}_k) + B\hat{g}(\hat{x}_k)u_k, \quad k_i \le k < k_{i+1} \quad \forall i \in \mathbb{N} \tag{14}$$

where $\hat{x}_k = [\hat{x}_{1,k} \ \hat{x}_{2,k} \ \cdots \ \hat{x}_{n,k}]^T \in \Re^n$ represents the estimated state vector. The functions $\hat{f}(\hat{x}_k) \in \Re$ and $\hat{g}(\hat{x}_k) \in \Re$ represent the approximation of the nonlinear functions $f(x_k)$ and $g(x_k)$, respectively. The system state vector, x_k, is available intermittently only at $k = k_i$, $\forall i \in \mathbb{N}$. Thus, the approximation of the nonlinear functions is expressed as $\hat{f}(\hat{x}_k)$ and $\hat{g}(\hat{x}_k)$ with the estimated state vector, $\hat{x}_k$. Furthermore, as proposed, the SE state vector is reinitialized as in (13).

The dynamics of the SE in (14), in an augmented form as in (3), for both inter-event times and event sampled instants using (13), can be represented as

$$\hat{x}_{k+1} = \begin{cases} A\hat{x}_k + B\hat{\bar{F}}(\hat{x}_k)\bar{u}_k, & k_i < k < k_{i+1} \\ Ax_k + B\hat{\bar{F}}(x_k)\bar{u}_k, & k = k_i \end{cases} \tag{15}$$

where $\hat{\bar{F}}(\hat{x}_k) = [\hat{f}(\hat{x}_k) \ \hat{g}(\hat{x}_k)]$ and $\hat{\bar{F}}(x_k) = [\hat{f}(x_k) \ \hat{g}(x_k)]$.

Consider the augmented system dynamics (3). The nonlinear function, $\bar{F}(x_k)$, can be approximated in the event sampled context, similar to (8) and (9), using the SE state $\hat{x}_k$ as input to the NN. Hence, $\bar{F}(x_k)$ can be expressed as

$$\bar{F}(x_k) = W^T\Phi(\hat{\bar{x}}_k) + \Xi_e(\hat{x}_k, e_k^s), \quad k_i \le k < k_{i+1} \quad \forall i \in \mathbb{N} \tag{16}$$

where $W = [W_f^T \ \ W_g^T]^T \in \Re^{2l\times 1}$ is the unknown target NN weight matrix with $W_f \in \Re^l$ and $W_g \in \Re^l$ represents the target weights for $f(x_k)$ and $g(x_k)$. The event-based activation function matrix is denoted by

$$\Phi(\hat{\bar{x}}_k) = \begin{bmatrix} \varphi_f\left(V_f^T \hat{x}_k\right) & 0_{l\times 1} \\ 0_{l\times 1} & \varphi_g\left(V_g^T \hat{x}_k\right) \end{bmatrix} \in \Re^{2l\times 2}$$

where $V_f \in \Re^{n\times l}$ and $V_g \in \Re^{n\times l}$ are randomly assigned constant weights at the input layers, and $\varphi_f(\cdot)$ and $\varphi_g(\cdot)$ represent the NN activation functions for f and g, respectively. The input matrices can be selected as $V_f = V_g = V$. Then, $\hat{\bar{x}}_k = V_f^T \hat{x}_k = V_g^T \hat{x}_k = V^T \hat{x}_k$. The event-based reconstruction error using the SE state vector is denoted by

$$\Xi_e\left(\hat{x}_k, e_k^s\right) = \Xi\left(\hat{x}_k + e_k^s\right) + W^T\left(\Phi\left(V^T\left(\hat{x}_k + e_k^s\right)\right) - \Phi\left(V^T\hat{x}_k\right)\right)$$

where $\Xi(\hat{x}_k + e_k^s) = \Xi(x_k) = [\varepsilon_f(x_k) \ \varepsilon_g(x_k)] \in \Re^{1\times 2}$ is the traditional reconstruction error in augmented form. The reconstruction errors $\varepsilon_f(x_k)$ and $\varepsilon_g(x_k)$ are the errors for the function f and g, respectively. The additional error term, as in the case of ZOH-based approximation in (9), is given by $W^T\Phi((V^T(\hat{x}_k + e_k^s)) - \Phi(V^T\hat{x}_k))$.

The actual NN estimation of the function, $\hat{\bar{F}}(x_k)$, with SE state, $\hat{x}_k$, can be written similar to (11) for $k_i \le k < k_{i+1}$ as

$$\begin{aligned} \hat{\bar{F}}(x_k) &= \hat{W}_k^T \Phi(\bar{x}_k) \\ &= \hat{W}_k^T \Phi(\hat{\bar{x}}_k) + \hat{W}_k^T\left(\Phi\left(V^T\left(\hat{x}_k + e_k^s\right)\right) - \Phi\left(V^T\hat{x}_k\right)\right) \end{aligned} \tag{17}$$

where $\hat{W}_k = [\hat{W}_{f,k}^T \ \ \hat{W}_{g,k}^T]^T \in \Re^{2l\times 1}$ represents the estimated NN weight vector and

$$\Phi(\bar{x}_k) = \begin{bmatrix} \varphi_f(V^T x_k) & 0_{l\times 1} \\ 0_{l\times 1} & \varphi_g(V^T x_k) \end{bmatrix}$$

is the augmented activation function with $\bar{x}_k = V^T x_k$.

Remark 1: The error term $\Phi(V^T(\hat{x}_k + e_k^s)) - \Phi(V^T\hat{x}_k)$, both in (16) and (17), is the result of the model state $\hat{x}_k$ as input to the activation function during $k_i < k < k_{i+1}$ instead of system state x_k. In the case of a traditional NN-based model [16], where the system state is used periodically, this error is not present. Since the activation functions are smooth functions, this error can be represented in terms of event-trigger error, e_k^s using the Lipschitz continuity as given next.

Assumption 2 [16]: The target weight vector W, the NN activation function $\Phi(\cdot)$, and the reconstruction error $\Xi(\cdot)$ are bounded above [16] satisfying $\|W\| \le W_{\max}$, $\|\Phi(\cdot)\| \le \Phi_{\max}$, and $\|\Xi(\cdot)\| \le \Xi_{\max}$, where $W_{\max}$, $\Phi_{\max}$, and $\Xi_{\max}$ are positive constants.

Assumption 3: The NN activation function $\Phi(\bar{x}_k)$ is Lipschitz continuous on a compact set for all $x_k \in \Omega_x$. Then, there exists a constant $L > 0$ such that $||\Phi(\bar{x}_k) - \Phi(\hat{\bar{x}}_k)|| \le L||\bar{x}_k - \hat{\bar{x}}_k|| \le L_\Phi||e_k^s||$ are satisfied, where $L_\Phi = L||V||$ is a constant.

The SE dynamics (15) by the NN approximation can be expressed as

$$\hat{x}_{k+1} = \begin{cases} A\hat{x}_k + B\hat{W}_k^T\Phi(\hat{\bar{x}}_k)\bar{u}_k, & k_i < k < k_{i+1} \\ Ax_k + B\hat{W}_k^T\Phi(\bar{x}_k)\bar{u}_k, & k = k_i. \end{cases} \tag{18}$$

The event-based control input with the estimated SE state vector, $\hat{x}_k$, and the SE dynamics (15) can be represented as

$$u_k = \begin{cases} (-\hat{f}(\hat{x}_k) + K\hat{x}_k)/\hat{g}(\hat{x}_k), & k_i < k < k_{i+1} \\ (-\hat{f}(x_k) + Kx_k)/\hat{g}(x_k), & k = k_i. \end{cases} \tag{19}$$

The control law using the approximated dynamics from (18) is given by

$$u_k = \begin{cases} \left(-\hat{W}_{f,k}^T\varphi_f(\hat{\bar{x}}_k) + K\hat{x}_k\right)/\hat{W}_{g,k}^T\varphi_g(\hat{\bar{x}}_k), & k_i < k < k_{i+1} \\ \left(-\hat{W}_{f,k}^T\varphi_f(\bar{x}_k) + Kx_k\right)/\hat{W}_{g,k}^T\varphi_g(\bar{x}_k), & k = k_i. \end{cases} \tag{20}$$

To ensure that the control law (20) is well-defined, i.e., $\hat{W}_{g_k}^T\varphi_g(\hat{\bar{x}}) \ne 0$ at all-time instants k, the estimate $\hat{g}(\hat{x}_k)$ is defined as

$$\hat{g}(\hat{x}_k) = \begin{cases} \hat{W}_{g,k}^T\varphi_g(\hat{\bar{x}}_k), & \hat{W}_{g,k}^T\varphi_g(\hat{\bar{x}}) \ge g_{\min} \\ \hat{W}_{g,k-1}^T\varphi_g(\hat{\bar{x}}_{k-1}), & \text{otherwise.} \end{cases} \tag{21}$$

The augmented function approximation error can be written from (16) and (17) as

$$\tilde{\bar{F}}(x_k) = \bar{F}(x_k) - \hat{\bar{F}}(x_k) = \tilde{W}_k^T\Phi(\bar{x}_k) + \Xi(x_k), \quad k_i \le k < k_{i+1} \tag{22}$$

where $\tilde{\bar{F}} = [\tilde{f} \ \ \tilde{g}]$ with $\tilde{f}(\cdot) = f(\cdot) - \hat{f}(\cdot)$ and $\tilde{g}(\cdot) = g(\cdot) - \hat{g}(\cdot)$ are the function approximation errors for f and g, respectively. The NN weight estimation error is denoted by $\tilde{W}_k = W - \hat{W}_k$.

B. Event-Trigger Error Dynamics and Aperiodic Update Law

The dynamics of the event-trigger error (12) using (3) and (15) for $k_i < k < k_{i+1}$ can be written as

$$\begin{aligned} e_{k+1}^s &= x_{k+1} - \hat{x}_{k+1} = Ax_k + B\bar{F}(x_k)\bar{u}_k - A\hat{x}_k - B\hat{\bar{F}}(\hat{x}_k)\bar{u}_k \\ &= Ae_k^s + B\tilde{\bar{F}}(x_k)\bar{u}_k + B(\hat{\bar{F}}(x_k) - \hat{\bar{F}}(\hat{x}_k))\bar{u}_k \\ &\qquad k_i < k < k_{i+1}. \end{aligned} \tag{23}$$

Recalling the event-based function approximation (17) and the augmented function approximation error (22), (23) can be expressed as

$$e_{k+1}^s = Ae_k^s + B\tilde{W}_k^T\Phi(\bar{x}_k)\bar{u}_k + B\Xi_k\bar{u}_k + B\hat{W}_k^T\tilde{\Theta}(\bar{x}_k, \hat{\bar{x}}_k)\bar{u}_k \tag{24}$$

for $k_i < k < k_{i+1}$, where $\tilde{\Theta}(\bar{x}_k, \hat{\bar{x}}_k) = \Phi(\bar{x}_k) - \Phi(\hat{\bar{x}}_k)$ and $\Xi_k \equiv \Xi(x_k)$ for brevity. Similarly, the event-trigger error dynamics at the trigger instants using (3) and (18) become

$$e_{k+1}^s = B\tilde{W}_k^T\Phi(\bar{x}_k)\bar{u}_k + B\Xi_k\bar{u}_k, \quad k = k_i. \tag{25}$$

To ensure the convergence of the NN weight estimation error, $\tilde{W}_k$, the NN weight update law in an event-triggered context is selected as

$$\hat{W}_k = \hat{W}_{k-1} + \frac{\gamma_k\alpha\Phi(\bar{x}_{k-1})\bar{u}_{k-1}e_k^{s^T}B}{1 + \|\Phi(\bar{x}_{k-1})\|^2\|\bar{u}_{k-1}\|^2} - \gamma_k\kappa\hat{W}_{k-1} \qquad k_{i-1} \le k < k_i \tag{26}$$

where $\alpha > 0$ is the learning rate and $\kappa > 0$ is sigma modification term similar to that in the traditional adaptive control [15]. The indicator function, γ_k, is defined as

$$\gamma_k = \begin{cases} 0, & \text{event is not triggered}, \quad k_{i-1} < k < k_i \\ 1, & \text{event is triggered}, \quad k = k_i. \end{cases} \tag{27}$$

The indicator function enables the NN weights to be updated once an event is triggered, i.e., $\gamma_k = 1$. The event-trigger error e_k^s is first used to update the NN weights in (26), and then reset to zero for the next trigger. As the trigger instants are aperiodic in nature, the NN weights are updated in a nonperiodic manner, as proposed. This saves the computation when compared with the traditional NN-based control approaches [16].

The update law (26) needs both x_{k_i-1} and x_{k_i} at the trigger instant k_i for updating the NN weights and to reset the model state. As proposed, both the current and previous state vectors are transmitted as a single packet at the trigger instants.

The NN weight estimation error dynamics using (26) and forwarding one time step ahead can be derived as

$$\tilde{W}_{k+1} = \tilde{W}_k - \frac{\gamma_k \alpha \Phi(\bar{x}_k)\bar{u}_k e_{k+1}^{s^T} B}{1 + \|\Phi(\bar{x}_k)\|^2 \|\bar{u}_k\|^2} + \gamma_k \kappa \hat{W}_k, \quad k_i \le k < k_{i+1}. \tag{28}$$

The convergence of the NN weight estimation error, $\tilde{W}_k$, requires the vector, $\Phi(\bar{x}_k)\bar{u}_k$, in (28), persistently exciting which is a well-known fact in traditional adaptive and NN-based control [15]–[16], [18]–[19]. For completeness, the definition of the PE condition is given.

Definition 1 ([18] Persistency of Excitation): A vector $\phi(x_k) \in \Re^n$ is said to be persistently exciting over an interval if there exist positive constants δ, c, d, and $k_d \ge 1$, such that

$$cI \le \sum_{k=k_d}^{k_d+\delta} \phi(x_k)\phi^T(x_k) \le dI \tag{29}$$

where I is the identity matrix.

Remark 2: A PE like condition for $\Phi(\bar{x}_k)\bar{u}_k$, can be achieved by adding an exploration noise to the control input [20]. This keeps the control input and, in turn, the system states away from zero. Furthermore, the activation function also satisfies PE and $0 < \Phi_{\min} \le \|\Phi(x_k)\| \le \Phi_{\max}$ holds.

Lemma 1: Consider the adaptive SE (18) and the control law (20). Suppose Assumptions 1 and 2 hold, the NN weights be initialized in a compact set and tuned by using (26), and the vector $\Phi(\bar{x}_k)\bar{u}_k$ satisfies the PE condition. Let k_0 be the initial trigger instant, k_p be the pth trigger instant for an integer p, and $N \ge k_p$ is an integer representing the time instant. Then, the NN weight estimation error $\tilde{W}_k$ is bounded for all time and will converge to the ultimate bound when $k_i > k_p$ or, alternatively, for all-time instants $k > k_0 + N$ provided the learning gains satisfy $0 < \alpha < 1/4$ and $0 < \kappa < 1/4$.

Proof: Refer to the Appendix.

Note that the ultimate bound can be made arbitrarily small by selecting the proper design parameters and the number of neurons, as discussed in Remark 5. Next, the main results are claimed.

IV. Event-Trigger Condition and Stability

In this section, the ultimate boundedness (UB) [16] of the closed-loop ETC system state vector and NN weight estimation error is presented by designing a suitable adaptive event-trigger condition.

A. Closed-Loop System Dynamics

The closed-loop dynamics of the ETC system can be derived by using (2) and (19). Consider the inter-event times, i.e., $k_i < k < k_{i+1}$, $\forall i \in \mathbb{N}$. The closed-loop dynamics can be written as

$$\begin{aligned} x_{k+1} &= Ax_k + Bf(x_k) + (Bg(x_k)(-\hat{f}(\hat{x}_k) + K\hat{x}_k)/\hat{g}(\hat{x}_k)) \\ &= A_c x_k + BKe_k^s + B\tilde{\bar{F}}(x_k)\bar{u}_k + B(\hat{\bar{F}}(x_k) - \hat{\bar{F}}(\hat{x}_k))\bar{u}_k. \end{aligned}$$

By using the NN estimation (17) and (18) and the function approximation error (22), the closed-loop dynamics become

$$\begin{aligned} x_{k+1} &= A_c x_k + BKe_k^s + B\tilde{W}_k^T \Phi(\bar{x}_k)\bar{u}_k + B\Xi_k \bar{u}_k + B\hat{W}_k^T \\ &\quad \times \tilde{\Theta}(\bar{x}_k, \hat{\bar{x}}_k)\bar{u}_k, \quad k_i < k < k_{i+1}. \end{aligned} \tag{30}$$

Similarly, at the trigger instants, $k = k_i$, $\forall i \in \mathbb{N}$, the closed-loop dynamics using (2), (3), (19), and (20) can be written as

$$x_{k+1} = A_c x_k + B\tilde{W}_k^T \Phi(\bar{x}_k)\bar{u}_k + B\Xi_k \bar{u}_k, \quad k = k_i. \tag{31}$$

Furthermore, the closed-loop dynamics of the SE can be derived by using (14) and (19) as

$$\hat{x}_{k+1} = \begin{cases} A_c \hat{x}_k, & k_i < k < k_{i+1} \\ A_c x_k, & k = k_i. \end{cases} \tag{32}$$

The flowchart in Fig. 3 shows the implementation of the adaptive MBETC scheme designed in Sections III and IV.

B. Main Results

In this section, we claim the main results by designing an adaptive event-trigger condition. The closed-loop stability of the adaptive MBETC is shown by evaluating a single Lyapunov function for both during the events or trigger instants and inter-event times. It is shown in [7] and [13] that the Lyapunov function need not monotonically decrease both during the inter-event and event times [7]. Due to the aperiodic NN weight update, it is shown that the Lyapunov function may increase during the inter-event times but remains bounded. It is further shown that the bound during the inter-event times converges to the ultimate value with the trigger of events; this is shown in Fig. 4.

Consider the event-trigger error (12). The events occur when the following condition, referred to as the event-trigger condition, given by:

$$D(\|e_k^s\|) > \mu_k^{\mathrm{ET}} \|x_k\| \tag{33}$$

is satisfied, where

$$\mu_k^{\mathrm{ET}} = \sqrt{\Gamma \sigma_{\min}(Q) / \left(8\|K\|^2 \|\Lambda_1\| + 8L_\Phi^2 \|\bar{u}_k\|^2 \|\hat{W}_k\|^2 \|\Lambda_1\|\right)}$$

denotes the threshold coefficient and $0 < \Gamma < 1$. The matrices Λ_1 and Q are positive definite matrices and satisfy the

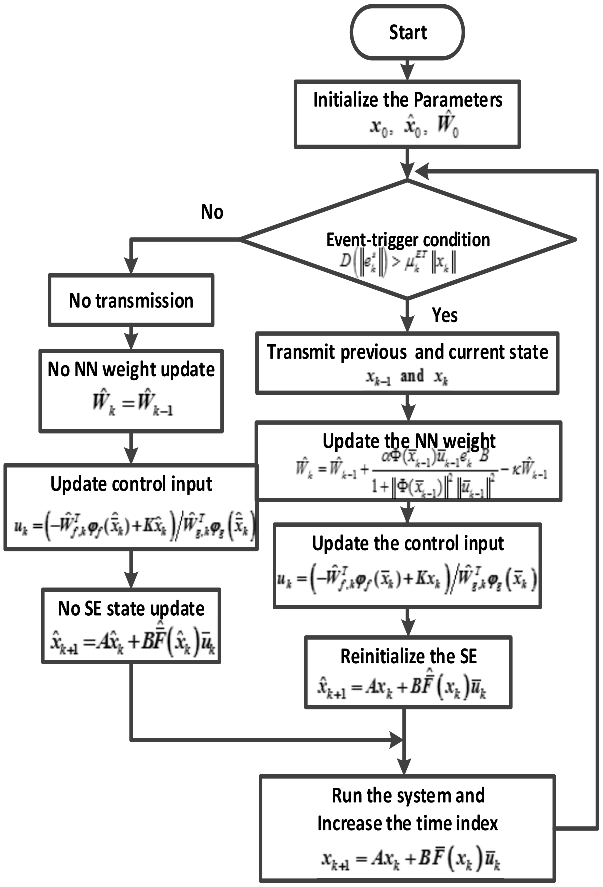

Fig. 3. Flowchart of the proposed ETC system.

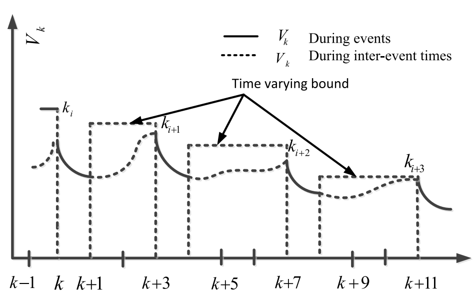

Fig. 4. Evolution of the Lyapunov function during event and inter-event times.

Lyapunov equation $\bar{A}_c^T \Lambda_1 \bar{A}_c - \Lambda_1 = -Q$ with $\bar{A}_c = \sqrt{2} A_c$, as shown in Remark A.1. The minimum singular value of Q is denoted by $\sigma_{\min}(Q)$. The dead-zone operator $D(\cdot)$ is defined as

$$D(\|e_k^s\|) = \begin{cases} \|e_k^s\|, & \text{if } \|x_k\| > B_x \\ 0, & \text{otherwise} \end{cases} \tag{34}$$

where B_x is the desired ultimate bound for the system state vector.

Remark 3: The threshold coefficient μ_k^{ET} in (33) is a function of the NN weight estimate, $\|\hat{W}_k\|$ and gets updated by (26). Therefore, the event-trigger condition (33) becomes adaptive. This helps in generating the required number of events for the function approximation during the learning phase of the NNs, as discussed in Section II-B1. Furthermore, μ_k^{ET} is also a function of the control gain K. The choice of control gain K is based on the desired closed-loop performance and the stability of the system such that $\bar{A}_c$ is Schur. This implies that the event-trigger condition is also driven by the system performance. Hence, for different choices of K, the trigger condition will ensure the required number of events to achieve the desired performance.

Remark 4: The dead-zone operator (34) is utilized in the event-trigger condition in order to reset the event-trigger error e_k^s to zero once the state vector is within the ultimate bound. This avoids unnecessary triggering of events due to the NN reconstruction error.

Theorem 1: Consider the nonlinear discrete-time system (1) along with the NN-based SE given in (18). Assume Assumptions 1–3 hold and the NN initial weight matrix $\hat{W}_0$ be initialized in a compact set. Suppose the system state vectors, x_{k_i} and x_{k_i-1}, are transmitted, the SE state vector, $\hat{x}_k$, is reinitialized, and the NN weights are updated using (26) as per the event-trigger condition (33). Let k_0 be the initial trigger instant, k_p be the pth trigger instant for any positive integer p, and $N \geq k_p$ is an integer represents the time instant. Then, the control input (20) ensures the closed-loop event-triggered system state vector, x_k, the SE state vector, $\hat{x}_k$, and the NN weight estimation error, $\tilde{W}_k$, are bounded for all time and converge to the ultimate bound for all trigger instants $k_i > k_p$ or, alternatively, for all $k > k_0 + N$ provided learning gains are selected, as shown in Lemma 1.

Proof: Refer to the Appendix.

Remark 5: From the proof of Theorem 1 (see the Appendix), the bounds on the system state vector, B_x, and NN weight estimation errors, $B_{\tilde{W}}$, depend upon the traditional NN reconstruction error, $\Xi_{\max}$, and the design parameters, α and κ. Through the proper selection of the number of neurons in the hidden layer and the design parameters α and κ, the bounds B_x and $B_{\tilde{W}}$ can be made arbitrarily small (see simulation results).

The minimum inter-event time, $\delta k_{\min} = \min_{i \in \mathbb{N}}(\delta k_i)$, where $\delta k_i = k_{i+1} - k_i$ for $i \in \mathbb{N}$, implicitly defined as the event-trigger condition (33), is the minimum time required for the event-trigger error, $\|e_k^s\|$, to evolve from zero and reach the event-trigger threshold, $\mu_k^{\mathrm{ET}}\|x_k\|$, over all inter-event times. In the case of a discrete-time system, which can be considered as discretized version of a continuous time system with a suitable fixed sampling time, trivially, the minimum inter-event time is the sampling time. Furthermore, in our case of model-based adaptive NN ETC, the minimum inter-event time may be one sampling time during the learning phase, but the inter-event times increase with the convergence of NN weight estimation error, thereby reducing the transmission.

V. Simulation Results

In this section, the proposed NN-based MBETC scheme is evaluated by using two examples.

Example 1: A second-order single-input and single-output nonlinear discrete-time system was selected for simulations whose dynamics are given as

$$\begin{aligned} x_{1,k+1} &= x_{2,k} \\ x_{2,k+1} &= f(x_k) + g(x_k) u_k \end{aligned} \tag{35}$$

where $f(x_k) = x_{2,k}/(1 + x_{1,k}^2)$ and $g(x_k) = 2 + \sin(x_{1,k})$.

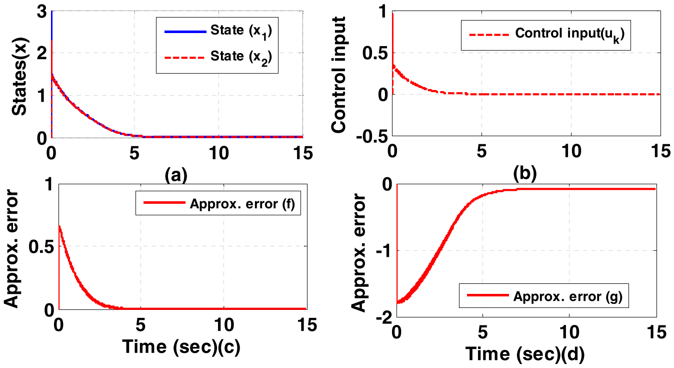

Fig. 5. Convergence of (a) state vector, (b) control input, (c) function approximation error $\tilde{f}(x_k)$, and (d) function approximation error $\tilde{g}(x_k)$.

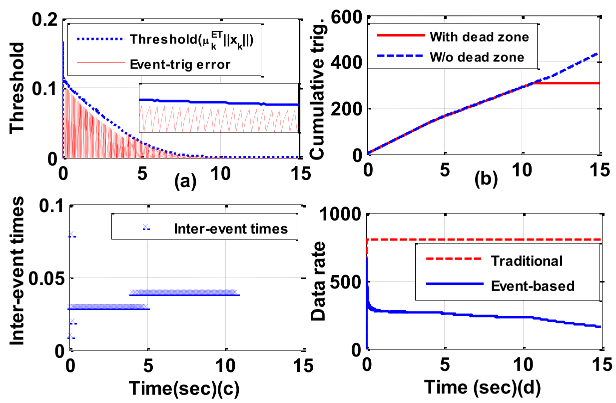

Fig. 6. Performance of the model-based adaptive NN ETC. (a) Evolution of event-trigger threshold and event-trigger error. (b) Cumulative number of trigger instants with and without dead-zone operator. (c) Inter-event time. (d) Comparison of the data rate between the traditional periodic transmission and the event-triggered transmission.

The following parameters were chosen during the simulation. The initial states of the system and the SE were selected to be $[3\ 2]^T$, since the first event is considered at k_0. Initial NN weights $V \in \Re^{2\times 15}$, $\hat{W}_{f,0} \in \Re^{15}$ and $\hat{W}_{g,0} \in \Re^{15}$ were chosen randomly from a uniform distribution in the interval [0, 1] with 15 neurons each in the hidden layers. The activation functions used were symmetric sigmoid functions ($\tanh(\cdot)$) for both the NNs with learning gains $\alpha = 0.24$ and $\kappa = 10^{-5}$. The control gain $K = [0.35\ 0.2]$ such that the matrix $\bar{A}_c = \sqrt{2}A_c$ is Schur. The event-trigger condition was derived from (33) with $g_{\min} = 1$ and $\Gamma = 0.99$. The Lipschitz constant L_Φ was computed as $L\|V\| = 3.28$ with $L = 1$. The system was simulated for 15 s. with a sampling time of 0.01 s, i.e., 1500 sampling instants. The ultimate bound for the system state vector was chosen to be 10^{-3}. The simulation results are shown in Figs. 5–7.

Fig. 5(a) shows the convergence of the system state vector close to zero with the event-based approximated control input in Fig. 5(b). The NN approximation errors of the nonlinear functions $f(x_k)$ and $g(x_k)$ are shown in Fig. 5(c) and (d), respectively. Due to NN initial weights being far away from the target, large initial errors are noticed in the plot, and finally, they converge to a bound close to zero. The boundedness

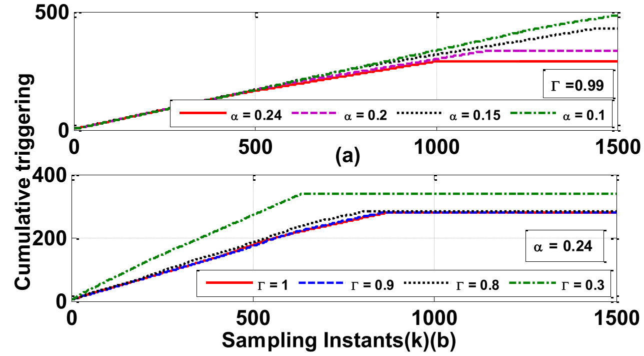

Fig. 7. Cumulative number of events with different values of (a) learning gain α and (b) event-trigger parameter Γ.

of these errors close to zero validated the event-based approximation discussed in Section II-A.

Next, the performance in terms of the triggering of events is shown in Figs. 6 and 7. Fig. 6(a) shows the evolution of the state-dependent event-trigger threshold and the error. The event-trigger error [see the zoomed-in view of Fig. 6(a)] resets to zero once the error reaches the threshold, and the system states were transmitted. Fig. 6(b) shows the count on the number of trigger instants that have occurred with respect to the total number of sampling instants. It was found that a total of 306 events occurred out of 1500 sampling instants. In addition, the plot indicates that the events are triggered frequently at the initial phase as a result of large approximation error resulting from the random initialization of NN weights. As the NN weights are updated and converge close to the target weights, the inter-event times increase. As expected, changing initial NN weights resulted in different numbers of events for the convergence of the weights.

The reduction in the number of cumulative events [the y-axis in Fig. 6(b)] demonstrates the effectiveness of the event-trigger scheme in reducing the number of state vector transmissions over the network in comparison with a traditional periodic sampled discrete-time control. The durations between two consecutive transmissions are shown in Fig. 6(c) and are aperiodic in nature. Assuming every packet size of 8 bit data, a comparison plot for the data rate in bits per second is shown in Fig. 6(d). In the case of the traditional discrete-time system, the data rate is constant, i.e., 800 b/s. In contrast, in the proposed ETC, the data rate reduces over time, since the transmissions are reduced and finally reaches to 100 b/s. This confirms a reduction in bandwidth usage and proves the effectiveness of the approach. Furthermore, the NN weights are updated 306 times, and thus reducing the computation for approximating the unknown nonlinear functions when compared with the traditional NN-based approach. However, the use of mirror adaptive SE for the evaluation of the event-trigger condition requires an additional computation.

A comparison between the trigger mechanisms with and without a dead-zone operator, in terms of cumulative number of event-trigger instants, is shown in Fig. 6(b). When the dead-zone operator is not used, as shown in Fig. 6(b) (dotted line), the events trigger continuously due to the NN reconstruction

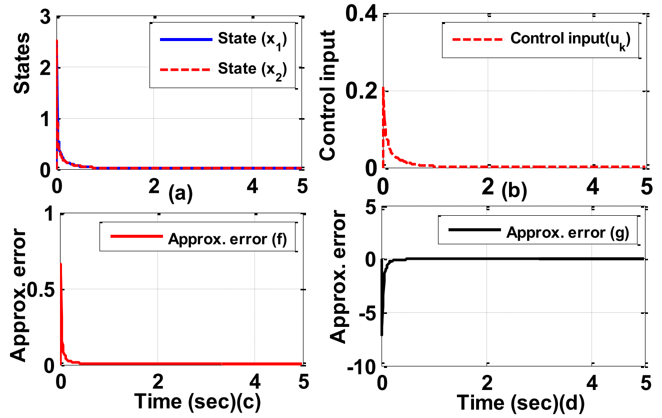

Fig. 8. Convergence of (a) state vector, (b) control input, (c) function approximation error $\tilde{f}(x_k)$, and (d) function approximation error $\tilde{g}(x_k)$.

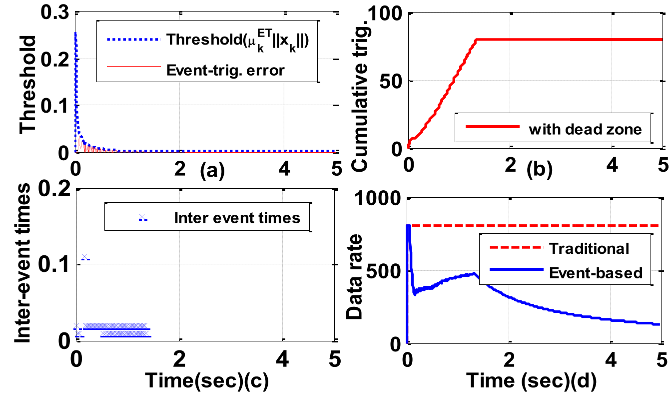

Fig. 9. Performance of the model-based adaptive NN ETC. (a) Evolution of event-trigger threshold and event-trigger error. (b) Cumulative number of trigger instants versus the total number of sampling instants. (c) Inter-event times. (d) Comparison of the data rate between the periodic transmission and the event-triggered transmission.

error even the system state vector is inside the ultimate bound. Hence, the dead-zone operator is necessary to reset the event-trigger error to zero once the state vector converge and stay inside the ultimate bound. This stops the unnecessary triggering of events, as shown in Fig. 6(b) (bold line).

Furthermore, the effect of different learning gains α and event-trigger parameters Γ on the number of events is shown in Fig. 7. As shown in Fig. 7(a), for different values of α, the cumulative number of events is different. This is due to the change in convergence rate of the NN weight updates. The number of cumulative triggers reduced with an increase in value Γ, since the threshold value increases with an increase in Γ. Note that Lyapunov stability is a sufficient condition. Therefore, the event-trigger threshold for $\Gamma = 1$ still maintains the stability of the system.

Example 2: In this example, another second-order system as in (35) was chosen where the system dynamics are given by $f(x_k) = x_{1,k}^2 x_{2,k}/(1 + x_{1,k}^2 + x_{2,k}^2)$ and $g(x_k) = 1 + (2/(1 + x_{1,k}^2 + x_{2,k}^2))$.

The simulation parameters were as follows. The initial values for the system and the SE states were $[1.5\ 2.5]^T$. The initial NN weights, $V \in \Re^{2\times 16}$, $\hat{W}_{f,0} \in \Re^{16}$, and $\hat{W}_{g,0} \in \Re^{16}$ were chosen randomly in the interval [0, 1] with 16 neurons each in the hidden layers. Symmetric sigmoid functions were used as the activation functions for both the NNs. Design parameters were selected as $\alpha = 0.24$, $\kappa = 10^{-5}$, $g_{\min} = 1$, $\Gamma = 0.99$, $L_\Phi = 3.6$, and $K = [0.3\ 0.25]$. The system was simulated for 5 s with a sampling time of 0.01 s, i.e., 500 sampling instants. The ultimate bound threshold of system state vector was chosen to be 8×10^{-3}.

The convergence of the system state and the control input is shown in Fig. 8(a) and (b), respectively. The NN approximation errors $\tilde{f}$ and $\tilde{g}$ are shown in Fig. 8(c) and (d), respectively. The cumulative number of triggers as shown in Fig. 9 (b) was observed to be 80 out of 500 sampling instants implying the saving in network resources and computation.

From both the examples, it is clear that the adaptive trigger condition is able to generate required number of triggers for the event-based function approximation with aperiodic update law. Furthermore, the reduction in the number of transmission verified the saving in communication bandwidth.

VI. Conclusion

In this paper, an NN-based adaptive ETC scheme for an uncertain nonlinear discrete-time system was introduced. An approximation of system dynamics by using NN was accomplished in the context of reduced event sampled communication. Two linearly parameterized NNs approximate the unknown nonlinear functions quite satisfactorily. The novel adaptive event-trigger condition ensured the stability and the desired performance of the complete uncertain system. In addition, the simulation results proved the efficacy of the proposed algorithm in terms of reducing the network traffic. It was observed that the number of triggered instants vary with the initial NN weights and the learning gain. Though a stabilizing controller was designed, it is not optimal. Hence, the design of the event-based optimal controller for uncertain systems will be as part of the future research.

Appendix

Proof of Lemma 1: The NN weights are updated only at the trigger instants and held during the inter-events times. Thus, the proof for the UB of the NN weight estimation error is carried out by evaluating a Lyapunov function candidate for both the cases as follows.

Case I [At the Trigger Instants ($k = k_i$, $\forall i \in \mathbb{N}$)]: Consider the Lyapunov function given by

$$V_{\tilde{W},k} = \mathrm{tr}\{\tilde{W}_k^T \tilde{W}_k\}. \tag{A.1}$$

The first difference, $\Delta V_{\tilde{W},k} = \mathrm{tr}\{\tilde{W}_{k+1}^T \tilde{W}_{k+1}\} - \mathrm{tr}\{\tilde{W}_k^T \tilde{W}_k\}$, along the weight estimation error dynamics (28) with the indicator function $\gamma_k = 1$ can be written as

$$\Delta V_{\tilde{W},k} = \mathrm{tr}\left\{\left(\tilde{W}_k - \frac{\alpha\Phi(\bar{x}_k)\bar{u}_k}{1 + \|\Phi(\bar{x}_k)\|^2\|\bar{u}_k\|^2} e_{k+1}^{sT} B + \kappa \hat{W}_k\right)^T \times \left(\tilde{W}_k - \frac{\alpha\Phi(\bar{x}_k)\bar{u}_k}{1 + \|\Phi(\bar{x}_k)\|^2\|\bar{u}_k\|^2} e_{k+1}^{sT} B + \kappa \hat{W}_k\right)\right\} - \mathrm{tr}\{\tilde{W}_k^T \tilde{W}_k\}.$$

Substitute the error dynamics in (25). Applying Cauchy–Schwartz (C–S) inequality with definitions $\hat{W}_k = W - \tilde{W}_k$ and $B^T B = 1$, the first difference satisfies

$$\begin{aligned}
&\Delta V_{\tilde{W},k} \\
&\quad \leq -\frac{\alpha}{1+\|\Phi(\bar{x}_k)\|^2\|\bar{u}_k\|^2}\mathrm{tr}\{\tilde{W}_k^T\Phi(\bar{x}_k)\bar{u}_k\bar{u}_k^T\Phi^T(\bar{x}_k)\tilde{W}_k\} \\
&\qquad + \frac{\alpha}{1+\|\Phi(\bar{x}_k)\|^2\|\bar{u}_k\|^2}\mathrm{tr}\{\Xi_k\bar{u}_k\bar{u}_k^T\Xi_k^T\} \\
&\qquad + 4\alpha^2\Psi\frac{\bar{u}_k^T\Phi^T(\bar{x}_k)\Phi(\bar{x}_k)\bar{u}_k}{(1+\|\Phi(\bar{x}_k)\|^2\|\bar{u}_k\|^2)^2} \\
&\qquad \times \mathrm{tr}\{(\tilde{W}_k^T\Phi(\bar{x}_k)\bar{u}_k)(\tilde{W}_k^T\Phi(\bar{x}_k)\bar{u}_k)^T\} - 2\kappa\mathrm{tr}\{\tilde{W}_k^T\tilde{W}_k\} \\
&\qquad + 4\kappa^2\mathrm{tr}\{W^TW\} + 4\kappa^2\mathrm{tr}\{\tilde{W}_k^T\tilde{W}_k\} + 2\kappa\mathrm{tr}\{\tilde{W}_k^TW\} \\
&\qquad + 4\alpha^2\frac{\bar{u}_k^T\Phi^T(\bar{x}_k)\Phi(\bar{x}_k)\bar{u}_k}{(1+\|\Phi(\bar{x}_k)\|^2\|\bar{u}_k\|^2)^2}\mathrm{tr}\{(\Xi_k\bar{u}_k)(\Xi_k\bar{u}_k)^T\}.
\end{aligned}$$

Observe that

$$\frac{\bar{u}_k^T\Phi^T(\bar{x}_k)\Phi(\bar{x}_k)\bar{u}_k}{1+\|\Phi(\bar{x}_k)\|^2\|\bar{u}_k\|^2} \leq \frac{\|\Phi(\bar{x}_k)\|^2\|\bar{u}_k\|^2}{1+\|\Phi(\bar{x}_k)\|^2\|\bar{u}_k\|^2} \leq 1.$$

Therefore, the first difference is upper bounded as

$$\begin{aligned}
&\Delta V_{\tilde{W},k} \\
&\quad \leq -\frac{\alpha(1-4\alpha)}{1+\|\Phi(\bar{x}_k)\|^2\|\bar{u}_k\|^2}\mathrm{tr}\{\tilde{W}_k^T\Phi(\bar{x}_k)\bar{u}_k\bar{u}_k^T\Phi^T(\bar{x}_k)\tilde{W}_k\} \\
&\qquad + \frac{\alpha(1+4\alpha)}{1+\|\Phi(\bar{x}_k)\|^2\|\bar{u}_k\|^2}\mathrm{tr}\{\Xi_k\bar{u}_k\bar{u}_k^T\Xi_k^T\} + 2\kappa\mathrm{tr}\{\tilde{W}_k^TW\} \\
&\qquad - 2\kappa\mathrm{tr}\{\tilde{W}_k^T\tilde{W}_k\} + 4\kappa^2\mathrm{tr}\{W^TW\} + 4\kappa^2\mathrm{tr}\{\tilde{W}_k^T\tilde{W}_k\}.
\end{aligned}$$

By using the inequality $2\mathrm{tr}\{A^TB\} \leq \|A\|^2 + \|B\|^2$ and Frobenius norm, the first difference leads to

$$\begin{aligned}
\Delta V_{\tilde{W},k} \leq{}& -\frac{\alpha(1-4\alpha)}{1+\|\Phi(\bar{x}_k)\|^2\|\bar{u}_k\|^2}\left\|\tilde{W}_k^T\Phi(\bar{x}_k)\bar{u}_k\right\|^2 + \kappa W_{\max}^2 \\
&+ \kappa\|\tilde{W}_k\|^2 - 2\kappa\|\tilde{W}_k\|^2 + 4\kappa^2W_{\max}^2 + 4\kappa^2\|\tilde{W}_k\|^2 \\
&+ \left(\alpha(1+4\alpha)\|\bar{u}_k\|^2\Xi_{\max}^2/(1+\|\Phi(\bar{x}_k)\|^2\|\bar{u}_k\|^2)\right).
\end{aligned}$$

Since $0 < \Phi_{\min} \leq \|\Phi(\bar{x}_k)\|$ is ensured by the PE condition, as discussed in Remark 2, the following inequality holds:

$$\begin{aligned}
&\frac{\|\bar{u}_k\|^2}{1+\|\Phi(\bar{x}_k)\|^2\|\bar{u}_k\|^2} \\
&\quad = \frac{\|\Phi(\bar{x}_k)\|^2\|\bar{u}_k\|^2}{(1+\|\Phi(\bar{x}_k)\|^2\|\bar{u}_k\|^2)\|\Phi(\bar{x}_k)\|^2} \leq \frac{1}{\Phi_{\min}^2}.
\end{aligned}$$

The first difference using the above inequality leads to

$$\begin{aligned}
\Delta V_{\tilde{W},k} \leq{}& -(\alpha(1-4\alpha)/(1+\|\Phi(\bar{x}_k)\|^2\|\bar{u}_k\|^2)) \\
&\times \left\|\tilde{W}_k^T\Phi(\bar{x}_k)\bar{u}_k\right\|^2 - \kappa(1-4\kappa)\|\tilde{W}_k\|^2 + B_M^{\tilde{W}}
\end{aligned}$$

where $B_M^{\tilde{W}} = (\alpha(1+4\alpha)\Xi_{\max}^2/\Phi_{\min}^2) + (\kappa+4\kappa^2)W_{\max}^2$ and $0 < \alpha < 1/4$. Dropping the first negative term, it holds that

$$\Delta V_{\tilde{W},k} \leq -\beta\|\tilde{W}_k\|^2 + B_M^{\tilde{W}}, \quad k = k_i \quad \forall i \in \mathbb{N} \tag{A.2}$$

where $\beta = \kappa(1-4\kappa) > 0$ by selecting $0 < \kappa < 1/4$. From (A.2), the first difference of the Lyapunov function, $\Delta V_{\tilde{W},k}$, is less than zero as long as $\|\tilde{W}_k\|^2 > B_M^{\tilde{W}}/\beta \equiv B_{\mathrm{UB}}^{\tilde{W}}$. Therefore, by using Lyapunov theorem [16], the NN weight estimation error $\tilde{W}_k$ is bounded at the trigger instants provided the vector $\Phi(\bar{x}_k)\bar{u}_k$ satisfies the PE condition.

Case II [During the Inter-event Times ($k_i < k < k_{i+1}$, $\forall i \in \mathbb{N}$)]:

Consider the Lyapunov function in (A.1). Along the NN weight estimation error dynamics (28) with $\gamma_k = 0$, the first difference of $V_{\tilde{W},k}$ can be expressed as

$$\begin{aligned}
\Delta V_{\tilde{W},k} &= \mathrm{tr}\{\tilde{W}_{k+1}^T\tilde{W}_{k+1}\} - \mathrm{tr}\{\tilde{W}_k^T\tilde{W}_k\} \\
&= \mathrm{tr}\{\tilde{W}_k^T\tilde{W}_k\} - \mathrm{tr}\{\tilde{W}_k^T\tilde{W}_k\} = 0.
\end{aligned} \tag{A.3}$$

From (A.3), the NN weight estimation error $\tilde{W}_k$ is a constant during the inter-event times. Since the NN weights are bounded at the trigger instants as demonstrated in Case I, and the initial weights are being finite, the weight estimation error, $\tilde{W}_k$, is bounded during the inter-event times.

From both the cases, we need to show that the NN weight estimation error converges to the ultimate bound. The first difference (A.2) in Case I for $k = k_i$ can be expressed as

$$\begin{aligned}
V_{\tilde{W},k_i+1} - V_{\tilde{W},k_i} &= \mathrm{tr}\{\tilde{W}_{k_i+1}^T\tilde{W}_{k_i+1}\} - \mathrm{tr}\{\tilde{W}_{k_i}^T\tilde{W}_{k_i}\} \\
&= \|\tilde{W}_{k_i+1}\|^2 - \|\tilde{W}_{k_i}\|^2 \leq -\beta\|\tilde{W}_{k_i}\|^2 + B_M^{\tilde{W}}.
\end{aligned}$$

Rearranging the above expression, one can express the above inequality as

$$\|\tilde{W}_{k_i+1}\| \leq (1-\beta)\|\tilde{W}_{k_i}\|^2 + B_M^{\tilde{W}}. \tag{A.4}$$

It is clear that $0 < 1-\beta < 1$ by the choice of $0 < \kappa < 1/4$. Furthermore, $\tilde{W}_k$, during the inter-event times, from (A.3) in Case II, remains constant. Thus, $\|\tilde{W}_{k_i}\| = \|\tilde{W}_{k_{i-1}+1}\|$ for $k_{i-1} < k < k_i$, $\forall i \in \mathbb{N}$. Therefore, (A.4) can be rewritten as

$$\|\tilde{W}_{k_i+1}\| \leq (1-\beta)\|\tilde{W}_{k_{i-1}+1}\|^2 + B_M^{\tilde{W}}. \tag{A.5}$$

Solving the difference inequality in (A.5) recursively, with the initial NN weight estimation error $\|\tilde{W}_{k_0}\| = \|\tilde{W}_0\| = B_{\tilde{W}0}$, the NN weight estimation error in (A.5) can be expressed as

$$\|\tilde{W}_{k_i+1}\|^2 \leq (1-\beta)^{i+1}B_{\tilde{W}0}^2 + ((1-(1-\beta)^{i+1}/\beta)B_M^{\tilde{W}} \equiv B_i^{\tilde{W}}. \tag{A.6}$$

Therefore, the constant upper bound on the NN weight estimation error during the inter-event times, from (A.6), is given by

$$\|\tilde{W}_k\|^2 \leq (1-\beta)^{i+1}B_{\tilde{W}0}^2 + ((1-(1-\beta)^{i+1}/\beta)B_M^{\tilde{W}} \equiv B_i^{\tilde{W}} \tag{A.7}$$

for $k_i < k < k_{i+1}$, $\forall i \in \mathbb{N}$.

The NN weights are initialized with a finite value, and the target weights are bounded. Therefore, the initial NN weight estimation error $\|\tilde{W}_{k_0}\| = \|\tilde{W}_0\| = B_{\tilde{W}0}$ is bounded. Furthermore, from (A.6), $B_i^{\tilde{W}}$ is a piecewise constant, converging sequence of functions since β satisfies $0 < \beta < 1$. Therefore, there exists an integer p (number of events) such that for the number of events $i > p$, the upper bound $B_i^{\tilde{W}}$ converges to the ultimate bound, i.e., $B_i^{\tilde{W}} \to B_{\mathrm{UB}}^{\tilde{W}}$ for all event-trigger instants $k_i > k_p$, where $B_{\mathrm{UB}}^{\tilde{W}} = B_M^{\tilde{W}}/\beta$ from (A.2).

Consequently, from Cases I and II, the NN weight estimation error $\tilde{W}_k$ is bounded for all-time instants and converges to the ultimate bound when $k_i > k_p$. Since k_i is a subsequence of k, the NN weight estimation error $\tilde{W}_k$ is UB for $k > k_0+N$, where $N \geq k_p$ is a positive integer. ■

Proof of Theorem 1: The proof of the theorem is completed by considering two cases, i.e., at the event-trigger instants and during the inter-event times. The first difference of the Lyapunov function is evaluated for both the cases, and finally combined to show the UB.

Case I [At the Trigger Instants ($k = k_i, \forall i \in \mathbb{N}$)]:

Consider the Lyapunov function candidate given as

$$V_k = V_{x,k} + \eta V_{\hat{x},k} + \varpi V_{A,k} + \Psi V_{\tilde{W},k} + \Pi V_{B,k} \quad \text{(A.8)}$$

where $V_{x,k} = x_k^T \Lambda_1 x_k$, $V_{\hat{x},k} = \hat{x}_k^T \Lambda_2 \hat{x}_k$, $V_{A,k} = (\hat{x}_k^T \Lambda_2 \hat{x}_k)^2$, $V_{\tilde{W},k} = \mathrm{tr}\{\tilde{W}_k^T \tilde{W}_k\}$, and $V_{B,k} = \mathrm{tr}\{\tilde{W}_k^T \tilde{W}_k\}^2$. The matrices Λ_1 and Λ_2 are the symmetric positive definite matrices and satisfy the Lyapunov equations $\bar{A}_c \Lambda_1 \bar{A}_c - \Lambda_1 = -Q$ and $A_c \Lambda_2 A_c - \Lambda_2 = -\bar{Q}$, where $\bar{A}_c = \sqrt{2} A_c$. The matrices Q and $\bar{Q}$ are the positive definite matrices. The constant coefficients are defined as $\eta = \max\{17\|K\|^2 \Xi_{\max}^2 \|\Lambda_1\|/g_{\min}^2 \times\sigma_{\min}(\bar{Q}), 9\|\Lambda_1\| \Xi_{\max}^2 \|K\|^2/g_{\min}^2 \sigma_{\min}(\bar{Q})\}$, $\varpi = \max\{9\|K\|^2 \times\|\Lambda_1\|\Phi_{\max}^2/\{g_{\min}^2 \sigma_{\min}(\bar{Q})\sigma_{\min}(A_c^T \Lambda_2 A_c + \Lambda_2)\}, 5\|\Lambda_1\|\|K\|^4/ g_{\min}^2 \sigma_{\min}(\bar{Q})\sigma_{\min}(A_c^T \Lambda_2 A_c + \Lambda_2)\}$, $\Psi = 2(4\Phi_{\max}^2\|\Lambda_1\| g_{\min}^2 +16\|\Lambda_1\|\Phi_{\max}^2(\Phi_{\max}^2 W_{\max}^2 + \Xi_{\max}^2))/g_{\min}^2 \beta$ and $\Pi = 42 \times\Phi_{\max}^4 \|\Lambda_1\|/\{g_{\min}^2 \beta(2-\beta)\}$ with $\sigma_{\min}(\cdot)$ is the minimum singular value.

For brevity, we will compute the first difference of each term in (A.8) individually and combine them at the final step to obtain the overall first difference.

Consider the first term, $V_{x,k} = x_k^T \Lambda_1 x_k$. The first difference along the system dynamics (31) can be expressed as

$$\begin{aligned}\Delta V_{x,k} &= \left[A_c x_k + B \tilde{W}_k^T \Phi(\bar{x}_k)\bar{u}_k + B \Xi_k \bar{u}_k\right]^T \Lambda_1 \\ &\quad\times\left[A_c x_k + B \tilde{W}_k^T \Phi(\bar{x}_k)\bar{u}_k + B \Xi_k \bar{u}_k\right] - x_k^T \Lambda_1 x_k.\end{aligned}$$

Applying C–S inequality, one can arrive at

$$\begin{aligned}\Delta V_{x,k} &\leq x_k^T \left(2A_c^T \Lambda_1 A_c - \Lambda_1\right)x_k + 4\left[B \tilde{W}_k^T \Phi(\bar{x}_k)\bar{u}_k\right]^T \Lambda_1 \\ &\quad\times\left[B \tilde{W}_k^T \Phi(\bar{x}_k)\bar{u}_k\right] + 4[B \Xi_k \bar{u}_k]^T \Lambda_1 [B \Xi_k \bar{u}_k] \\ &\leq -\sigma_{\min}(Q)\|x_k\|^2 + 4\Phi_{\max}^2\|\Lambda_1\|\|\tilde{W}_k\|^2\|\bar{u}_k\|^2 \\ &\quad+ 4\|\Lambda_1\|\|\bar{u}_k\|^2 \Xi_{\max}^2\end{aligned}$$

where $2A_c^T \Lambda_1 A_c - \Lambda_1 = -Q$ and $\|B\| = 1$.

Remark A.1: The Lyapunov equation $\bar{A}_c^T \Lambda_1 \bar{A}_c - \Lambda_1 = -Q$ has a positive definite solution only when the matrix $\bar{A}_c = \sqrt{2} A_{\boldsymbol{c}}$ is Schur. As per the definition of matrix $A_{\boldsymbol{c}}$ in (5), the control gain K can be selected to ensure $\bar{A}_c$ is Schur.

By using the facts $\varphi_{f,\max} \leq \Phi_{\max}$ and $\|W_{f,k}\| \leq \|W_k\|$, the control input at the trigger instants given in (20) satisfies

$$\begin{aligned}\|\bar{u}_k\|^2 &= 1 + \|u_k\|^2 \\ &= 1 + \left\|\left[-\hat{W}_{f,k}^T \varphi_f(\bar{x}_k) + K x_k\right]/\hat{W}_{g,k}^T \varphi_g(\bar{x}_k)\right\|^2 \\ &\leq 1 + \frac{4\Phi_{\max}^2 W_{\max}^2}{g_{\min}^2} + \frac{4\Phi_{\max}^2}{g_{\min}^2}\|\tilde{W}_k\|^2 + \frac{2\|K\|^2}{g_{\min}^2}\|x_k\|^2.\end{aligned} \quad \text{(A.9)}$$

Substituting inequality (A.9) and separating the cross product term using Young's inequality, $2ab \leq a^2 + b^2$, the first difference is bound by

$$\begin{aligned}\Delta V_{x,k} &\leq -\sigma_{\min}(Q)\|x_k\|^2 + 4\Phi_{\max}^2\|\Lambda_1\|\|\tilde{W}_k\|^2 \\ &\quad+ \left(16/g_{\min}^2\right)\Phi_{\max}^4 W_{\max}^2\|\Lambda_1\|\|\tilde{W}_k\|^2 \\ &\quad+ \left(20/g_{\min}^2\right)\Phi_{\max}^4\|\Lambda_1\|\|\tilde{W}_k\|^4 + \left(4/g_{\min}^2\right)\|\Lambda_1\| \\ &\quad\times\|K\|^4\|x_k\|^4 + \left(16/g_{\min}^2\right)\|\Lambda_1\|\Phi_{\max}^2 \Xi_{\max}^2 W_{\max}^2 \\ &\quad+ \left(16/g_{\min}^2\right)\|\Lambda_1\|\Phi_{\max}^2 \Xi_{\max}^2\|\tilde{W}_k\|^2 + \left(8/g_{\min}^2\right) \\ &\quad\times\|\Lambda_1\|\Xi_{\max}^2\|K\|^2\|x_k\|^2 + 4\|\Lambda_1\|\Xi_{\max}^2.\end{aligned} \quad \text{(A.10)}$$

Considering the second term of the Lyapunov function $V_{\hat{x},k} = \hat{x}_k^T \Lambda_2 \hat{x}_k$, the first difference along the closed-loop SE dynamics (32), with $\hat{x}_k = x_k$ at $k = k_i$, becomes

$$\begin{aligned}\Delta V_{\hat{x},k} &= \hat{x}_{k+1}^T \Lambda_2 \hat{x}_{k+1} - \hat{x}_k^T \Lambda_2 \hat{x}_k \\ &= (A_c x_k)^T \Lambda_2 (A_c x_k) - x_k^T \Lambda_2 x_k \\ &= x_k^T \left(A_c^T \Lambda_2 A_c - \Lambda_2\right)x_k \\ &= -x_k^T \bar{Q} x_k \leq -\sigma_{\min}(\bar{Q})\|x_k\|^2.\end{aligned} \quad \text{(A.11)}$$

Moving on for the third term, $V_{A,k} = (\hat{x}_k^T \Lambda_2 \hat{x}_k)^2$, the first difference $\Delta V_{A,k} = (\hat{x}_{k+1}^T \Lambda_2 \hat{x}_{k+1})^2 - (\hat{x}_k^T \Lambda_2 \hat{x}_k)^2$ can be written as $\Delta V_{A,k} = \Delta V_{\hat{x},k}(\Delta V_{\hat{x},k} + 2x_k^T \Lambda_2 \boldsymbol{x}_k)$. Substituting $\Delta V_{\hat{x},k}$ from (A.11) reveals that

$$\Delta V_{A,k} \leq -\sigma_{\min}(\bar{Q})\sigma_{\min}\left(A_c^T \Lambda_2 A_c + \Lambda_2\right)\|x_k\|^4. \quad \text{(A.12)}$$

Now, the first difference of the fourth term $V_{\tilde{W},k}$ in the Lyapunov function can be written from (A.2) in Lemma 1 and given by

$$\Delta V_{\tilde{W},k} \leq -\beta\|\tilde{W}_k\|^2 + B_M^{\tilde{W}}. \quad \text{(A.13)}$$

Considering the last term $V_{B,k} = \mathrm{tr}\{\tilde{W}_k^T \tilde{W}_k\}^2$, the first difference can be computed using (A.13) as follows:

$$\begin{aligned}\Delta V_{B,k} &= \left(\mathrm{tr}\left\{\tilde{W}_{k+1}^T \tilde{W}_{k+1}\right\}^2 - \mathrm{tr}\left\{\tilde{W}_k^T \tilde{W}_k\right\}^2\right) \\ &\leq \left(-\beta\|\tilde{W}_k\|^2 + B_M^{\tilde{W}}\right)\left((2-\beta)\|\tilde{W}_k\|^2 + B_M^{\tilde{W}}\right).\end{aligned}$$

Appling Young's inequality $2ab \leq pa^2 + (b^2/p)$ reveals that

$$\Delta V_{B,k} \leq -(1/2)\beta(2-\beta)\|\tilde{W}_k\|^4 + (((2-\beta)/2\beta) + 1)\left(B_M^{\tilde{W}}\right)^2 \quad \text{(A.14)}$$

where $(2-\beta) > 0$ by the selection of $0 < \kappa < 1/4$.

Finally, combining all the individual first differences given in (A.10)–(A.14), the overall first difference $\Delta V_k = \Delta V_{x,k} + \eta\Delta V_{\hat{x},k} + \varpi\Delta V_{A,k} + \Psi\Delta V_{\tilde{W},k} + \Pi\Delta V_{B,k}$, with η, ϖ, Ψ, and Π from (A.8), found to be

$$\begin{aligned}\Delta V_k &\leq -\sigma_{\min}(Q)\|x_k\|^2 - \left(1/g_{\min}^2\right)\|\Lambda_1\|\Xi_{\max}^2\|K\|^2\|x_k\|^2 \\ &\quad- \left(4\Phi_{\max}^2\|\Lambda_1\| + \frac{16}{g_{\min}^2}\|\Lambda_1\|\Phi_{\max}^2 \times\left(\Phi_{\max}^2 W_{\max}^2 + \Xi_{\max}^2\right)\right)\|\tilde{W}_k\|^2 \\ &\quad- \left(1/g_{\min}^2\right)\|\Lambda_1\|\|K\|^4\|x_k\|^4 \\ &\quad- \left(1/g_{\min}^2\right)\Phi_{\max}^4\|\Lambda_1\|\|\tilde{W}_k\|^4 + B_{TM}^{c2}\end{aligned} \quad \text{(A.15)}$$

where $B_{TM}^{c2} = (16/g_{\min}^2)\|\Lambda_1\|\Phi_{\max}^2 \Xi_{\max}^2 W_{\max}^2 + 4\|\Lambda_1\|\Xi_{\max}^2 + \Psi B_M^{\tilde{W}} + \Pi(((2-\beta)/2\beta) + 1)(B_M^{\tilde{W}})^2$.

From (A.15), the Lyapunov first difference ΔV_k is less than zero as long as

$$\|x_k\| > \max\left\{\sqrt{B_{TM}^{c2}/\sigma_{\min}(Q)}, \sqrt{g_{\min}^2 B_{TM}^{c2}/\|\Lambda_1\|\Xi_{\max}^2\|K\|^2}, \sqrt[4]{g_{\min}^2 B_{TM}^{c2}/\|\Lambda_1\|\|K\|^4}\right\} \equiv B_{1,M}^x$$

or

$$\|\tilde{W}_k\| > \max \times\left\{\sqrt{\frac{g_{\min}^2 B_{TM}^{c2}}{\{4\Phi_{\max}^2 g_{\min}^2\|\Lambda_1\| + 16\|\Lambda_1\|\Phi_{\max}^2(\Phi_{\max}^2 W_{\max}^2 + \Xi_{\max}^2)\}}}, \sqrt[4]{g_{\min}^2 B_{TM}^{c2}/\Phi_{\max}^4\|\Lambda_1\|}\right\} \equiv B_{1,M}^{\tilde{W}}.$$

Therefore, by using the Lyapunov theorem [16], the system state x_k, the SE state $\hat{x}_k$, and the NN weight estimation error $\tilde{W}_k$ are bounded at the trigger instants. Furthermore, when $i > p$ or, alternatively, all trigger instants $k_i > k_p$, where p is an integer representing the events, the system state x_k, the SE state $\hat{x}_k$, and the NN weight estimation error $\tilde{W}_k$ are all ultimately bounded.

Case II [During the Inter-event Times ($k_i < k < k_{i+1}$, $\forall i \in \mathbb{N}$)]:

Consider the Lyapunov function given in (A.8) in Case I. Similar to Case I, we will evaluate the individual terms separately. Note that the NN weights are not updated during the inter-event times and held at their previous values.

Consider the first term $V_{x,k} = x_k^T \Lambda_1 x_k$ of the Lyapunov function candidate (A.8). The first difference $\Delta V_{x,k}$ along the closed-loop system trajectory (30) can be expressed as

$$\begin{aligned}\Delta V_{x,k} &= x_{k+1}^T \Lambda_1 x_{k+1} - x_k^T \Lambda_1 x_k \\ &= \big[A_c x_k + BKe_k^s + B\tilde{W}_k^T \Phi(\bar{x}_k)\bar{u}_k \\ &\quad + B\Xi_k \bar{u}_k + B\hat{W}_k^T \tilde{\Theta}(\bar{x}_k, \hat{\bar{x}}_k)\bar{u}_k\big]^T \\ &\quad \times \Lambda_1\big[A_c x_k + BKe_k^s + B\tilde{W}_k^T \Phi(\bar{x}_k)\bar{u}_k \\ &\quad + B\Xi_k \bar{u}_k + B\hat{W}_k^T \tilde{\Theta}(\bar{x}_k, \hat{\bar{x}}_k)\bar{u}_k\big] - x_k^T \Lambda_1 x_k.\end{aligned}$$

Applying C–S inequality, the first difference can be represented as

$$\begin{aligned}\Delta V_{x,k} \le& -x_k^T Q x_k + 8\big(B\tilde{W}_k^T \Phi(\bar{x}_k)\bar{u}_k\big)^T \Lambda_1\big(B\tilde{W}_k^T \Phi(\bar{x}_k)\bar{u}_k\big) \\ &+ 8(B\Xi_k\bar{u}_k)^T \Lambda_1 (B\Xi_k \bar{u}_k) \\ &+ 4\big[BKe_k^s + B\hat{W}_k^T \tilde{\Theta}(\bar{x}_k, \hat{\bar{x}}_k)\bar{u}_k\big]^T \\ &\times \Lambda_1\big[BKe_k^s + B\hat{W}_k^T \tilde{\Theta}(\bar{x}_k, \hat{\bar{x}}_k)\bar{u}_k\big]\end{aligned}$$

where Q satisfies the Lyapunov equation $\bar{A}_c^T \Lambda_1 \bar{A}_c - \Lambda_1 = -Q$ with $\bar{A}_c = \sqrt{2}A_c$. By using Frobenius norm and triangle inequality with the fact $\|B\| = 1$ reveals

$$\begin{aligned}\Delta V_{x,k} \le& -\sigma_{\min}(Q)\|x_k\|^2 + 8\Phi_{\max}^2\|\tilde{W}_k\|^2\|\bar{u}_k\|^2\|\Lambda_1\| + 8\|\bar{u}_k\|^2 \\ &\times \|\Lambda_1\|\|\Xi_k\|^2 + 4\big\|BKe_k^s + B\hat{W}_k^T \tilde{\Theta}(\bar{x}_k, \hat{\bar{x}}_k)\bar{u}_k\big\|^2\|\Lambda_1\|.\end{aligned}$$

Applying C–S and Young's inequalities and replacing $\|\tilde{\Theta}(\bar{\boldsymbol{x}}_k, \hat{\bar{\boldsymbol{x}}}_k)\| \le L\|\bar{\boldsymbol{x}}_k - \hat{\bar{\boldsymbol{x}}}_k\| \equiv L_\Phi\|e_k^s\|$ from Assumption 3, the first difference is expressed as

$$\begin{aligned}\Delta V_{x,k} \le& -\sigma_{\min}(Q)\|x_k\|^2 + 8\Phi_{\max}^2\|\tilde{W}_k\|^2\|\bar{u}_k\|^2\|\Lambda_1\| \\ &+ 8\|K\|^2\|e_k^s\|^2\|\Lambda_1\| + 8L_\Phi^2\|\hat{W}_k\|^2\|e_k^s\|^2\|\bar{u}_k\|^2\|\Lambda_1\| \\ &+ 8\|\bar{u}_k\|^2\|\Lambda_1\|\|\Xi_k\|^2. \end{aligned} \tag{A.16}$$

By definition of the control input (20) for $k_i < k < k_{i+1}$, the following inequality holds:

$$\|\bar{u}_k\|^2 \le 1 + \frac{4\Phi_{\max}^2 W_{\max}^2}{g_{\min}^2} + \frac{4\Phi_{\max}^2}{g_{\min}^2}\|\tilde{W}_k\|^2 + \frac{2\|K\|^2}{g_{\min}^2}\|\hat{x}_k\|^2. \tag{A.17}$$

Substituting (A.17) in the first difference (A.16) and with simple mathematical manipulation, one can reach at

$$\begin{aligned}\Delta V_{x,k} \le& -\sigma_{\min}(Q)\|x_k\|^2 + \big(16/g_{\min}^2\big)\|K\|^2\Xi_{\max}^2\|\Lambda_1\|\|\hat{x}_k\|^2 \\ &+ \big(8/g_{\min}^2\big)\|K\|^2\|\Lambda_1\|\|\hat{x}_k\|^4\Phi_{\max}^2 \\ &+ \big(8\|K\|^2\|\Lambda_1\| + 8L_\Phi^2\|\hat{W}_k\|^2\|\bar{u}_k\|^2\|\Lambda_1\|\big)\|e_k^s\|^2 \\ &+ 8\Phi_{\max}^2\|\Lambda_1\|\big(1 + \big(4/g_{\min}^2\big)\big(\Phi_{\max}^2 W_{\max}^2 + \Xi_{\max}^2\big)\big) \\ &\times\|\tilde{W}_k\|^2 + \big(8/g_{\min}^2\big)\Phi_{\max}^2\|\Lambda_1\|\|\tilde{W}_k\|^4\big(4\Phi_{\max}^2 + \|K\|^2\big) \\ &+ 32\big(\Phi_{\max}^2/g_{\min}^2\big)\|\Lambda_1\|W_{\max}^2\Xi_{\max}^2 + 8\|\Lambda_1\|\Xi_{\max}^2.\end{aligned}$$

Recall the event-trigger condition (33). During the inter-event times, for the case when the system state vector is outside the ultimate bound, it holds that $\|e_k^s\| \le \mu_k^{\mathrm{ET}}\|x_k\|$. Using this inequality and substituting μ_k^{ET} from (33) into the above first difference and one can arrive at

$$\begin{aligned}\Delta V_{x,k} \le& -(1-\Gamma)\sigma_{\min}(Q)\|x_k\|^2 + \big(16/g_{\min}^2\big)\|K\|^2\Xi_{\max}^2\|\Lambda_1\| \\ &\times\|\hat{x}_k\|^2 + 8\Phi_{\max}^2\|\Lambda_1\|\|\tilde{W}_k\|^2 \\ &\times\big(1 + \big(4/g_{\min}^2\big)\big(\Phi_{\max}^2 W_{\max}^2 + \Xi_{\max}^2\big)\big) \\ &+ \big(8/g_{\min}^2\big)\|K\|^2\|\Lambda_1\|\Phi_{\max}^2\|\hat{x}_k\|^4 \\ &+ \big(8/g_{\min}^4\big)\Phi_{\max}^2\|\Lambda_1\|\|\tilde{W}_k\|^4 \\ &\times\big(4\Phi_{\max}^2 + \|K\|^2\big) + \big(8\|\Lambda_1\| \\ &+ \big(32/g_{\min}^4\big)\Phi_{\max}^2 W_{\max}^2\|\Lambda_1\|\big)\Xi_{\max}^2. \end{aligned} \tag{A.18}$$

Consider the second term $V_{\hat{x},k} = \hat{x}_k^T \Lambda_2 \hat{x}_k$ of the Lyapunov function (A.8). The first difference $\Delta V_{\hat{x},k}$ along the closed-loop SE dynamics (32) for $k_i < k < k_{i+1}$ can be represented as

$$\begin{aligned}\Delta V_{\hat{x},k} = \hat{x}_{k+1}^T \Lambda_2 \hat{x}_{k+1} - \hat{x}_k^T \Lambda_2 \hat{x}_k &= -\hat{x}_k^T \bar{Q}\hat{x}_k \\ &\le -\sigma_{\min}(\bar{Q})\|\hat{x}_k\|^2 \end{aligned} \tag{A.19}$$

where the positive definite matrix $\bar{Q}$ satisfies the Lyapunov equation $A_c^T \Lambda_2 A_c - \Lambda_2 = -\bar{Q}$.

The first difference of the third term $V_{A,k} = (\hat{x}_k^T \Lambda_2 \hat{x}_k)^2$ can be written using (A.19) as

$$\begin{aligned}\Delta V_{A,k} &\le -\hat{x}_k^T \bar{Q}\hat{x}_k\big(-\hat{x}_k^T \bar{Q}\hat{x}_k + 2\hat{x}_k^T \Lambda_2 \hat{x}_k\big) \\ &\le -\sigma_{\min}(\bar{Q})\sigma_{\min}\big(A_c^T \Lambda_2 A_c + \Lambda_2\big)\|\hat{x}_k\|^4. \end{aligned} \tag{A.20}$$

The first difference of the fourth term, $V_{\tilde{W},k} = \mathrm{tr}\{\tilde{W}_k^T \tilde{W}_k\}$, in (A.8) can be written from (A.3) and given as

$$\Delta V_{\tilde{W},k} = 0. \tag{A.21}$$

Therefore, the first difference of $V_{B,k} = \operatorname{tr}\{\tilde{W}_k^T \tilde{W}_k\}^2$ from (A.21) is written as

$$\Delta V_{B,k} = 0. \tag{A.22}$$

The overall first difference, $\Delta V_k = \Delta V_{x,k} + \eta \Delta V_{\hat{x},k} + \varpi \Delta V_{A,k} + \Psi \Delta V_{\tilde{W},k} + \Pi \Delta V_{B,k}$, by combining (A.18)–(A.22), and recalling the definition of η and ϖ, is upper bounded by

$$\Delta V_k \le -\sigma_{\min}(Q)(1-\Gamma)\|x_k\|^2 - \left(1/g_{\min}^2\right)\Phi_{\max}^2\|K\|^2\|\Lambda_1\| \times \|\hat{x}_k\|^4 - \left(1/g_{\min}^2\right)\|K\|^2\,\Xi_{\max}^2\|\Lambda_1\|\|\hat{x}_k\|^2 + B_{\Xi}^M + B_{\tilde{W},i}^M \tag{A.23}$$

where $B_{\Xi}^M = (8\|\Lambda_1\| + (32/g_{\min}^4)\Phi_{\max}^2 W_{\max}^2\|\Lambda_1\|)\Xi_{\max}^2$ and $B_{\tilde{W},i}^M = 8\Phi_{\max}^2\|\Lambda_1\|(1 + (4/g_{\min}^2)(\Phi_{\max}^2 W_{\max}^2 + \Xi_{\max}^2))B_i^{\tilde{W}} + (8\Phi_{\max}^2\|\Lambda_1\|/g_{\min}^2)(4\Phi_{\max}^2 + \|K\|^2)B_i^{\tilde{W}^2}$ with $B_i^{\tilde{W}}$ is piecewise constant bound of $\tilde{W}_k$ for the ith inter-event time from Lemma 1. From (A.23), the overall first difference ΔV_k is less than zero as long as

$$\|x_k\| > \sqrt{(B_{\Xi}^M + B_{\tilde{W},i}^M)/\sigma_{\min}(Q)(1-\Gamma)} \equiv B_{2,i}^x$$

or

$$\|\hat{x}_k\| > \max\left\{\sqrt{\left(B_{\Xi}^M + B_{\tilde{W},i}^M\right)g_{\min}^2/\|K\|^2\,\Xi_{\max}^2\|\Lambda_1\|},\ \sqrt[4]{\left(B_{\Xi}^M + B_{\tilde{W},i}^M\right)g_{\min}^2/\|K\|^2\|\Lambda_1\|\Phi_{\max}^2}\right\} \equiv B_{2,i}^{\hat{x}}.$$

This implies either the system state vector outside the ball of radius $B_{2,i}^x$ or the SE state vector outside the ball of radius $B_{2,i}^{\hat{x}}$, both will converge to their respective bounds in a finite time. Since inter-event times are followed by the trigger instants, the initial values of x_k, $\hat{x}_k$, and $\tilde{W}_k$, during the inter-event times, are the updated values from the trigger instants. It is shown in Case I that x_k, $\hat{x}_k$, and $\tilde{W}_k$, are bounded at the trigger instants. Therefore, the system and SE state vectors are bounded during the inter-event times. Note that the function $B_{\tilde{W},i}^M$ in (A.23) is a piecewise constant function, since $B_i^{\tilde{W}}$ in (A.7), from Lemma 1, is constant during the ith inter-event time. Therefore, the bounds for the system and the SE state vectors, $B_{2,i}^x$, and $B_{2,i}^{\hat{x}}$, respectively, are piecewise constant functions.

During the initial learning phase of the NN, the upper bound on the NN weight estimation error $B_i^{\tilde{W}}$ in (A.7) may be large. Hence, the piecewise constant function $B_{\tilde{W},i}^M$ and in turn $B_{2,i}^x$ and $B_{2,i}^{\hat{x}}$ are of larger value. The system and SE state vectors inside the ball of radius $B_{2,i}^x$ and $B_{2,i}^{\hat{x}}$, respectively, may increase within these bounds. It follows that the Lyapunov function (A.8) may increase and bounded by the piecewise constant bound. The upper bound on the Lyapunov function using the upper bounds of the system state, the SE state, and the NN weight estimation error can be expressed as

$$V_k \le B_{1,i}^{x^2} + \eta B_{2,i}^{\hat{x}^2} + \varpi B_{2,i}^{\hat{x}^4} + \Psi B_i^{\tilde{W}} + \Pi B_i^{\tilde{W}^2} \tag{A.24}$$

for $k_i < k < k_{i+1}$, $\forall i \in \mathbb{N}$.

To show the UB of x_k, $\hat{x}_k$, and $\tilde{W}_k$, we need to show the functions $B_{\tilde{W},i}^M$, $B_{2,i}^x$, and $B_{2,i}^{\hat{x}}$ converge to their ultimate values. The bounds $B_{\tilde{W},i}^M$, $B_{2,i}^x$, and $B_{2,i}^{\hat{x}}$ are the functions of $B_i^{\tilde{W}}$. Since $B_i^{\tilde{W}}$ in (A.7) is a converging sequence, shown in Lemma 1, and converges to $B_{\text{UB}}^{\tilde{W}}$ for all $i > p$, the function $B_{\tilde{W},i}^M$ in (A.23) converges to the ultimate value, i.e., $B_{\tilde{W},i}^M \to B_{\tilde{W},M}^M$ for all $i > p$, where $B_{\tilde{W},M}^M = 8\Phi_{\max}^2\|\Lambda_1\| \times (1 + (4/g_{\min}^2)(\Phi_{\max}^2 W_{\max}^2 + \Xi_{\max}^2))B_{\text{UB}}^{\tilde{W}} + (8\Phi_{\max}^2\|\Lambda_1\|/g_{\min}^2)(4\Phi_{\max}^2 + \|K\|^2)B_{\text{UB}}^{\tilde{W}^2}$. Consequently, the bounds $B_{2,i}^x \to B_{2,M}^x$ and $B_{2,i}^{\hat{x}} \to B_{2,M}^{\hat{x}}$ for all $i > p$, where

$$B_{2,M}^x = \sqrt{(B_{\Xi}^M + B_{\tilde{W},M}^M)/\sigma_{\min}(Q)(1-\Gamma)}$$

and

$$B_{2,M}^{\hat{x}} = \max\left\{\sqrt{\left(B_{\Xi}^M + B_{\tilde{W},M}^M\right)g_{\min}^2/\|K\|^2\,\Xi_{\max}^2\|\Lambda_1\|},\ \sqrt[4]{\left(B_{\Xi}^M + B_{\tilde{W},M}^M\right)g_{\min}^2/\|K\|^2\|\Lambda_1\|\Phi_{\max}^2}\right\}.$$

Therefore, combining results from Cases I and II, the system state x_k, the SE state $\hat{x}_k$, and the NN weight estimation error $\tilde{W}_k$ are bounded for all time and converge to the ultimate bound when $i > p$ or with events occurring such that $k_i > k_p$. Therefore, all the closed-loop system signals are UB for all time $k > k_0 + N$, since k_i is a subsequence of k, where $N \ge k_p$ represents the time instant.

From both the cases of the proof and Lemma 1, the bounds for the system state vector, the SE state vector, and the NN weight estimation error can be selected as $B_x = \max(B_{1,M}^x, B_{2,M}^x)$, $B_{\hat{x}} = \max(B_{1,M}^x, B_{2,M}^{\hat{x}})$, and $B_{\tilde{W}} = \max(B_{\text{UB}}^{\tilde{W}}, B_{2,M}^{\tilde{W}})$, respectively.

Remark A.2: It is routine to check that for the case $|\hat{g}(\hat{x}_k)| < g_{\min}$, in (21), the first differences in (A.15) and (A.23) also hold. Therefore, with similar arguments, the closed-loop event-triggered system is ultimately bounded. ■

References

[1] K. J. Astrom and B. M. Bernhardsson, "Comparison of Riemann and Lebesgue sampling for first order stochastic systems," in *Proc. 41st IEEE Conf. Decision Control*, vol. 2. Las Vegas, NV, USA, Dec. 2002, pp. 2011–2016.

[2] P. Tabuada, "Event-triggered real-time scheduling of stabilizing control tasks," *IEEE Trans. Autom. Control*, vol. 52, no. 9, pp. 1680–1685, Sep. 2007.

[3] M. C. F. Donkers and W. P. M. H. Heemels, "Output-based event-triggered control with guaranteed $\mathcal{L}_\infty$-gain and improved and decentralized event-triggering," *IEEE Trans. Autom. Control*, vol. 57, no. 6, pp. 1362–1376, Jun. 2012.

[4] J. Lunze and D. Lehmann, "A state-feedback approach to event-based control," *Automatica*, vol. 46, no. 1, pp. 211–215, Jan. 2010.

[5] C. Stocker and J. Lunze, "Event-based control of nonlinear systems: An input-output linearization approach," in *Proc. 50th IEEE Conf. Decision Control Eur. Control Conf.*, Orlando, FL, USA, Dec. 2011, pp. 2541–2546.

[6] E. Garcia and P. J. Antsaklis, "Model-based event-triggered control for systems with quantization and time-varying network delays," *IEEE Trans. Autom. Control*, vol. 58, no. 2, pp. 422–434, Feb. 2013.

[7] X. Wang and M. D. Lemmon, "On event design in event-triggered feedback systems," *Automatica*, vol. 47, no. 10, pp. 2319–2322, Oct. 2011.

[8] W. P. M. H. Heemels and M. C. F. Donkers, "Model-based periodic event-triggered control for linear systems," *Automatica*, vol. 49, no. 3, pp. 698–711, Mar. 2013.

[9] X. Wang and N. Hovakimyan, "$\mathcal{L}_\infty$ adaptive control of event-triggered networked systems," in *Proc. Amer. Control Conf.*, Baltimore, MD, USA, Jun./Jul. 2010, pp. 2458–2463.

[10] A. Sahoo, H. Xu, and S. Jagannathan, "Adaptive event-triggered control of a uncertain linear discrete time system using measured input and output data," in *Proc. Amer. Control Conf.*, Washington, DC, USA, Jun. 2013, pp. 5692–5697.

[11] A. Sahoo, H. Xu, and S. Jagannathan, "Neural network-based adaptive event-triggered control of affine nonlinear discrete time systems with unknown internal dynamics," in *Proc. Amer. Control Conf.*, Washington, DC, USA, Jun. 2013, pp. 6418–6423.

[12] A. Sahoo, H. Xu, and S. Jagannathan, "Near optimal event-based control of nonlinear discrete time systems in affine form with measured input and output data," in *Proc. Int. Joint Conf. Neural Netw.*, Beijing, China, Jul. 2014, pp. 3671–3676.

[13] H. Ye, A. N. Michel, and L. Hou, "Stability theory for hybrid dynamical systems," *IEEE Trans. Autom. Control*, vol. 43, no. 4, pp. 461–474, Apr. 1998.

[14] A. Yeşildirek and F. L. Lewis, "Feedback linearization using neural networks," *Automatica*, vol. 31, no. 11, pp. 1659–1664, 1995.

[15] K. S. Narendra and A. M. Annaswamy, *Stable Adaptive Systems*. New York, NY, USA: Dover, 2005.

[16] J. Sarangapani, *Neural Network Control of Nonlinear Discrete-Time Systems*. Boca Raton, FL, USA: CRC Press, 2006.

[17] M. Green and J. B. Moore, "Persistence of excitation in linear systems," *Syst. Control Lett.*, vol. 7, no. 5, pp. 351–360, Sep. 1986.

[18] G. C. Goodwin and K. S. Sin, *Adaptive Filtering Prediction and Control*. New York, NY, USA: Dover, 2009.

[19] D. Gorinevsky, "On the persistency of excitation in radial basis function network identification of nonlinear systems," *IEEE Trans. Neural Netw.*, vol. 6, no. 5, pp. 1237–1244, Sep. 1995.

[20] H. Xu, S. Jagannathan, and F. L. Lewis, "Stochastic optimal control of unknown linear networked control system in the presence of random delays and packet losses," *Automatica*, vol. 48, no. 6, pp. 1017–1030, Jun. 2012.

Avimanyu Sahoo received the B.S. degree in electrical technology from the Cochin University of Science and Technology, Cochin, India, in 2008, and the M.S. degree in electrical engineering from IIT Varanasi, Varanasi, India, in 2011. He is currently pursuing the Ph.D. degree with the Department of Electrical Engineering, Missouri University of Science and Technology, Rolla, MO, USA.

His current research interests include event sampled control, adaptive control, neural network control, networked control system, and optimal control.

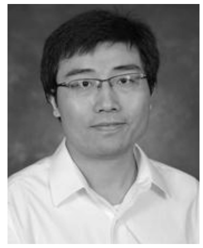

Hao Xu (M'12) was born in Nanjing, China, in 1984. He received the master's degree in electrical engineering from Southeast University, Nanjing, in 2009, and the Ph.D. degree from the Missouri University of Science and Technology, Rolla, MO, USA, in 2012.

He is currently with Texas A&M Corpus Christi, Corpus Christi, TX, USA, where he is an Assistant Professor with the College of Science and Engineering and the Director of the Unmanned Systems Research Laboratory. His research interests included autonomous unmanned aircraft systems, wireless passive sensor network, localization, detection, networked control system, cyber-physical system, distributed network protocol design, optimal control, and adaptive control.

Sarangapani Jagannathan (SM'00) is currently with the Missouri University of Science and Technology, Rolla, MO, USA, where he is a Rutledge-Emerson Endowed Chair Professor of Electrical and Computer Engineering and the Site Director of the NSF Industry/University Cooperative Research Center on Intelligent Maintenance Systems. He supervised to graduation around 19 Ph.D. and 29 M.S. level students and his funding is in excess of U.S. \$14.5 million from various U.S. federal and industrial members. He has co-authored 134 peer-reviewed journal articles, most of them in the IEEE TRANSACTIONS, 238 refereed IEEE conference articles, several book chapters, three books, and holds 20 U.S. patents. His current research interests include neural network control, adaptive event-triggered control, secure networked control systems, prognostics, and autonomous systems/robotics.

Dr. Jagannathan is a fellow of the Institute of Measurement and Control in U.K., and the Institution of Engineering and Technology in U.K. He received many awards and has been on organizing committees of several IEEE conferences. He was the Co-Editor of the *IET Book Series* in control from 2010 to 2013, and serves as the Editor-in-Chief of *Discrete Dynamics in Nature and Society* and on many editorial boards. He is the IEEE CSS Tech Committee Chair on Intelligent Control.